Polymer-Based Low-Temperature Thermoelectric Composites

Khabib Yusupov* and Alberto Vomiero*

Thermoelectric materials allow direct conversion of waste heat energy into electrical energy, thus contributing to solving energy related issues. Polymer-based materials have been considered for use in heat conversion in the temperature range from 20 to 200 °C, within which conventional materials are not efficient enough, whereas polymers due to their good electronic transport properties, easy processability, non-toxicity, flexibility, abundance, and simplicity of adjustment, are considered as promising materials. Due to the large variety of available polymers and the almost unlimited combinations of possible modifications, the field of polymer-based thermoelectrics is very rapidly developing, already reaching efficiency values close to those of inorganic systems. In the current progress report, the most recent advances in the field are discussed. New approaches to improve thermoelectric performance are described, with a focus on revising the mechanisms to improve the thermoelectric properties of the three most investigated polymer matrixes: poly(3,4-ethylenedioxythiophene) polystyrene sulfonat, poly(3-hexylthiophene-2,5-diyl), and polyaniline, alongside the three main paths of optimizing properties: incorporation of carbon-based material and inorganic substances, and treatment with chemical agents. The most promising research in the field is highlighted and thoroughly analyzed. The path toward a lab-to-fab transition for thermoelectric polymers is suggested in perspective.

1. Introduction

Energy in all its forms is one of the most valuable entities in our era, being one of the foundations of our society: economy (manufactures), communications (airplanes, cars, etc.), electricity in daily use and many others.[1] Considering that the population of the earth is around seven billion people (keeps growing [2]) and that the consumption of
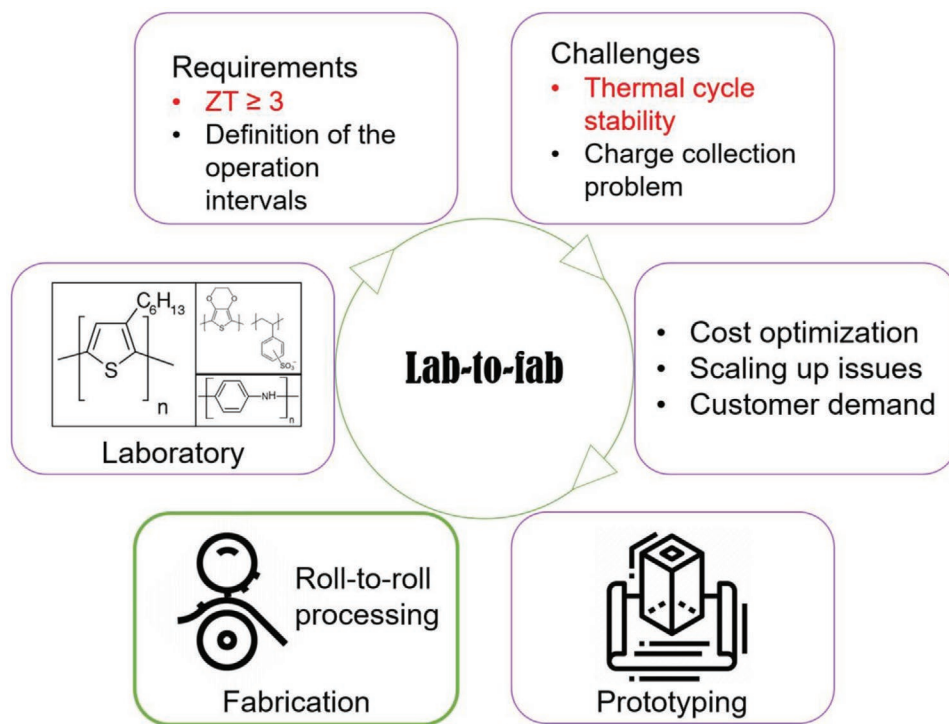
Dr. K. Yusupov, Prof. A. Vomiero
Division of Materials Science
Department of Engineering Sciences and Mathematics
Luleå University of Technology
Luleå 97187, Sweden
E-mail: khabib.yusupov@ltu.se; alberto.vomiero@ltu.se,
alberto.vomiero@unive.it

Prof. A. Vomiero
Department of Molecular Sciences and Nanosystems
Ca' Foscari University of Venice
Via Torino 155, Venezia Mestre 30172, Italy

The ORCID identification number(s) for the author(s) of this article can be found under https://doi.org/10.1002/adfm.202002015.

energy per person is increasing continuously, the problem of energy delivery, will keep growing. This is the main driving force to work on exploring efficient and new sources of energy. An environmentally friendly[3,4] solution to the energy problem is the target of the present research. Among renewable sources, wind,[5] already used both on the ground and off shore, biomass,[6] and solar energy[7,8] can be named. Such sources, while environmentally non harmful, still cannot fulfill the ever-growing energy needs. An additional source of energy, which can be used, is the dissipated heat. According to Vallero,[9] the heat dissipation from the global use of non-renewable energy has resulted in an additional net heat source. It should be added that also renewable sources produce waste heat. Recycling the waste heat energy should lead to a partial solution of the energy problem. The use of thermoelectric (TE) materials (especially low-T and flexible TE) can play a role in new and low energy consumption application such as portable sensors and wearable electronics.[10]

The best way to use the waste heat energy is the thermoelectric effect, more specifically the Seebeck effect, which allows converting heat into electricity.[11–13] When a temperature difference is applied to the opposite sides of a material, a potential difference occurs, which enables the flow of charge carriers in a close circuit, that is, electric current. The evaluation of TE materials is estimated by the dimensionless figure-of-merit $ZT = (\sigma \cdot S^2)/k \cdot T$, where S is the Seebeck coefficient, σ and k are the electrical and thermal conductivities, respectively, and T is the absolute temperature. In some cases, the performance of TE materials is measured by using only the numerator (PF, power factor) of the previous equation, when it is not possible to estimate k. The highest efficiency can be reached only at high values for the PF and low values of k.

Over the years, thermoelectric materials have not been used widely but the need for energy and breakthroughs in this field allowed the TE materials to become thoroughly investigated. Conventionally, inorganic semiconductors are used for TE application.[14] Though the highest values of ZT were achieved for those type of materials, they have some disadvantages, such as high thermal conductivity due to the intrinsic nature of the materials, resembling metals, processing difficulties, cost, toxicity (for some) and others.[11] The major heat lost is within the temperature range from 20 and 400 °C making this range the target for research filed. After the discovery of conductivity in polymers by Shirakawa et al.,[15] polymers became a promising

**ADVANCED
SCIENCE NEWS**

www.advancedsciencenews.com

**ADVANCED
FUNCTIONAL
MATERIALS**

www.afm-journal.de

Scheme 1. Simplified version of Lab-to-fab process for TE materials.

alternative materials for low-temperature TE. This aspect, together with a broad perspective on the subject, is emphasized in the recent review works.[16–18] The reviews are focusing on describing the modern research works, the most promising among them and news approaches for boosting TE performance. However, they focus less on the main mechanisms behind the improvements of transport properties, whereas here it is one of the main discussions.

Though conductive polymers have advantages (low thermal conductivity, flexibility, etc.), they also have some drawbacks, such as low values of the Seebeck coefficient, to overcome. A variety of ways have been pursued to improve TE performance, such as the incorporation of organic[19] or inorganic[20] fillers, treatment of polymer by chemical agents during or after their synthesis,[21] synthesis of new polymers[22] and others. The goal ZT of 3 (and possibly higher) is one of the major steps for future implementation of the TE technology. However, for an effective lab-to-fab transition other important features have to be guaranteed by the proposed technology. The simplified representation of lab-to-fab is shown in the **Scheme 1**.

For a successful manufacturing of the TE materials, ZT values higher than 3 for the selected operating temperature range has to be achieved. Other challenges to be overcome relate the long-term stability of the TE performance and optimal process of collection of charge carriers through the electrodes. The stability tests can be performed via two different procedures: i) exposure of the material to the temperature difference for 10 000 h and ii) thermal cycling (over 10 000). At present there is no consensus about the stability tests; however, there is a criticism of the second procedure which highlights that the dimensions of the materials should be counted

with thermal cycling.[23] Further steps in the lab-to-fab process include optimization of the manufacturing process to decrease the expenses of the materials production; solving the issue of scaling up the materials so the TE performance remains or growth with the increasing size of the samples; adjusting the production volume according to the customer demand; creating a prototype if necessary, that is especially applicable for the flexible and uncommonly shaped devices. The final step is an actual Fabrication. One should mainly focus on the two main points of the lab-to-fab process, which are ZT ≥ 3 and stability. These two characteristics are the most challenging and essential characteristics of the future TE generators, being responsible for the TE performance and the time of usage. The current progress report is focused on recent research related to TE materials based on polymer matrixes. A variety of conductive[24,25] and non-conductive polymers[26,27] have been used in the TE field. Polymers represent the new frontier in the research for efficient TE materials due to their valuable and suitable properties.[28] Among all the polymers, the present progress report focuses on the three mainly used for TE application: poly(3,4-ethylenedioxythiophene) polystyrene sulfonate (PEDOT:PSS), poly(3-hexylthiophene-2,5-diyl) (P3HT), and polyaniline (PANI). The chosen polymers are modified via different approaches such as organic/inorganic filler incorporation, exposure to the chemical agents, mechanical stresses, and adjustment of the composition. In the progress report different mechanisms behind the improvement are thoroughly investigated. We aim at filling the lack of systematic studies in the field, collecting the most recent literature in the field, and suggesting future avenues for the successful exploitation of this class of composite advanced materials.

2. PEDOT:PSS

PEDOT:PSS is based on highly conductive and hydrophobic PEDOT chains and insulating and hydrophilic PSS chains as a stabilizer for the conductive part. The combination of these two components synergizes the electrical conductivity and water dispersibility. Despite its transport properties, PEDOT: PSS is not perfectly suitable for TE application due to the intrinsically low values of its electrical conductivity ($\approx$1 S cm^{-1}) and Seebeck coefficient ($\approx$20 μV K^{-1}). For these reasons, strong efforts have been put to improve its TE performance. The main strategies of doing so are thoroughly described below. As mentioned in the introduction, the goal ZT value for commercialization of all TE materials is 3 and higher. However, achieving high ZT values is still a major challenge: the current highest and stable ZT value for polymer TE is $\approx$0.7. All values close or exciding it, should be counted as valuable, and indicative of a promising material in the field."

2.1. Integration of Carbon-Based Materials

PEDOT:PSS itself is widely used for various electronic applications. However, the PSS part of the polymeric system being an insulator, is known to highly decrease the electronic transport properties. Thus, various studies focused on the replacement of the PSS part with other counter ions. In this section the polymers obtained by PEDOT in combination with counterions other than PSS, implementing carbon-based materials (carbon nanotubes, graphene oxide, etc.) will be described. Carbon-based materials are chosen due to their exceptional electronic transport properties and nanodimensions, which makes them useful and attractive candidates as fillers in polymers. However, utilization of carbon-based materials per se is not the most efficient approach in improving the TE performance. To boost up the performance additional steps apart

from filler incorporation are required to either complement and support filler contribution or to create a synergetic effect from a few simultaneous approaches. The main among them are chemical treatments (redox processes), as shown by Choi et al.,[29] where the description of PEDOT:tosylate (tos) polymer synthesis on top of the single-walled carbon nanotubes (CNTs) with further redox process (tetrakis (dimethylamino)ethylene) was the main focus. A remarkable increase of the Seebeck coefficient from 44 μV K^{-1} to 14 mV K^{-1} after 30 min chemical treatment was observed. The concentration of single-walled carbon nanotubes (SWCNTs) directly affects the results of the chemical treatment: at high SWCNT concentration, the chemical treatment induces a decrease of thermopower and an increase of electrical conductivity due to the formation of SWCNTs percolated network. The highest PF and figure-of-merit of $\approx$1200 μW mK^{-2} and 0.4, respectively, were achieved for a medium level of filler incorporation. The increase of the Seebeck coefficient is explained by the improvement of charge carrier mobility and the contribution of ions, that is, Soret effect[30] (**Figure 1**a), when the redox process was carried out at a 60% relative humidity, which is known to promote dissociation and mobility of ions.

In turn, the work by Kim et al.[31] focused on the creation of p- and n-type fibers based on PEDOT:PSS and CNTs for TE generators. The fibers were obtained via direct spinning of preliminarily prepared paste made from polymer, filler and distilled/deionized water. By immersing fibers into aqueous hydrazine solution, the thermopower of the fibers ($\approx$45 μV K^{-1}) was improved, and higher concentration of CNTs induced the change of electronic behavior of fibers from p- to n-type conductivity. The p- to n-type doping transition via hydrazine treatment (Figure 1b) is explained by the n-type doping of CNT via hydrazine, that is, an improvement in electronic charge carrier density managed to overcome the density of holes. Further treatment of n-type fibers with polyethyleneimine (PEI) increased the TE performance since PEI acts as a high electron
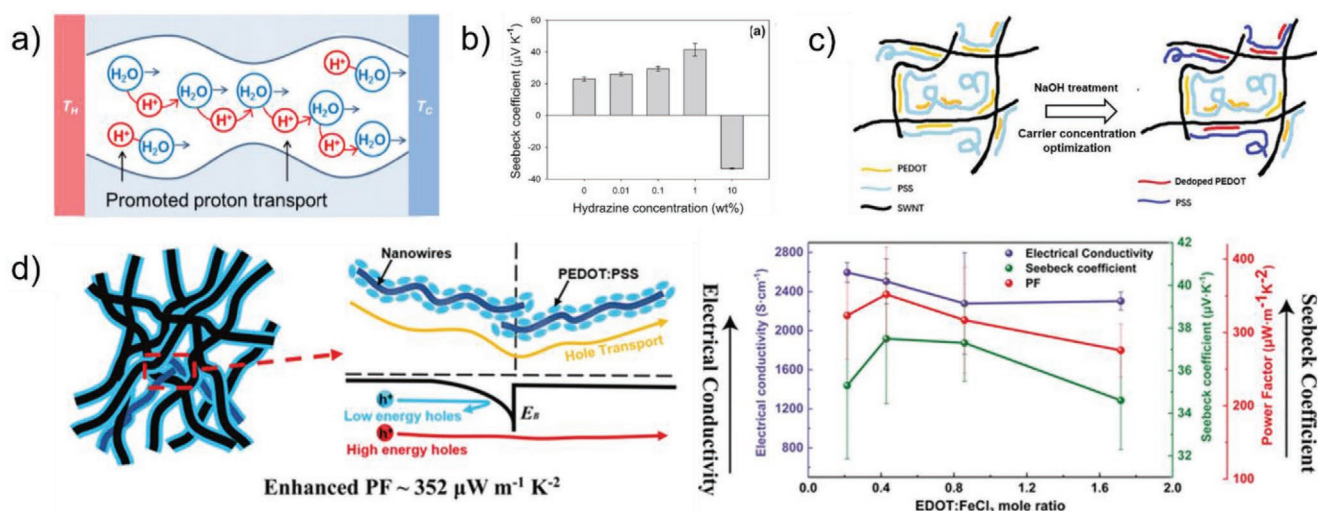

Figure 1. a) Soret effect, that is, migration of ions through a material driven by a temperature gradient. Reproduced with permission.[30] Copyright 2017, Elsevier Ltd. b) Change from p- to n-type conductivity via hydrazine treatment. Reproduced with permission.[31] Copyright 2018, Elsevier Ltd. c) Dedoping mechanism via NaOH treatment. Reproduced with permission.[34] Copyright 2019, Elsevier Ltd. d) Scheme of energy filtering mechanism and its influence on TE performance. Reproduced with permission.[37] Copyright 2019, American Chemical Society.

donor on the surface of CNTs. The highest PF for p- and n-type fibers reached 83 and 113 µW mK^{-2}, respectively.

In ref. [32], we used a vertically aligned forest of multi-walled CNTs (CNTF) as filler. The core of the research consisted in the preparation of a tape of aligned CNTs on an insulating glassy substrate, further covered by a polymer, by varying the number of CNT layers and the sequence of CNT deposition/polymer impregnation. We reached almost 3-fold improvement of PF compared to the polymer without CNT addition, up to ≈57 µW mK^{-2}. We also investigated[33] the influence on the same system of the post-treatment process by dimethyl sulfoxide (DMSO) and ethylene glycol (EG) on TE performance. The post-treatment process led to partial removal and rearrangement/delocalization of the insulating PSS part, which improved transport properties for the system. The highest PF, 92 µW mK^{-2}, is achieved for the sample with EG post-treatment and a single layer structure. Multilayered samples exhibit smaller increase in functionality, since the chemical post-treatment results less effective. In this respect, the research highlighted an issue, still unsolved, for preparation of multi-layered materials, where the chemical treatment is uneven along film depth, due to the screening effect of the top layers. Overall, the best performing system showed ≈fivefold improvement of PF compared to a pure PEDOT:PSS film.

The application of SWCNTs is usually associated to higher functionalities due to the superior transport properties compared to multi-walled carbon nanotubes (MWCNTs). Such results were achieved by Li and co-workers,[34] where SWCNT were used as filler content, which allowed achieving simultaneous increase of electrical conductivity and Seebeck coefficient, which are typically mutually exclusive properties. Improved functionality is associated with parallel-connected two-component mixture model,[35] where the presence of SWCNT with high Seebeck coefficient decreases the concentration of charge carriers in polymer, at low SWCNT concentration, then, with increased SWCNT concentration, the electrical conductivity improves, leading to the highest PF values of 298 µW mK^{-2} for 60 wt % concentration of SWCNTs. Successive treatment with 0.1 M NaOH base led to an increase of the Seebeck coefficient, and a decrease of the electrical conductivity from 32 to 56 µV K^{-1} and from 2685 to 1216 S cm^{-1}, respectively, with the highest PF equal to 526 µW mK^{-2}. Further treatment led to the decrease of both the properties. The simultaneous improvement is explained by the change of doping and oxidation level (Figure 1c). Na ions "deactivated" the PSS part of the polymer, which reduced the amount of charge carriers, thus improving their mobility. It is estimated that the base treatment led to change of the polymer structure from quinoid to low conductive benzoid one. The ZT values of manufactured samples are in the range from 0.26 to 0.39. These values were calculated by the authors by combining their own experimental results on electrical conductivity and Seebeck coefficient, and tabulated values for thermal conductivity taken from ref. [36].

One of the mechanisms to boost TE performance of the polymer composites is an energy filtering mechanism (EFM),[38,39] that is, the presence of an energy barrier at the phase interface of various compounds. The energy barrier is working as a "filter" system, where only charge carriers with enough energy can pass through, resulting in a decreased concentration of the charge carriers and in nominally increased entropy.

As an outcome of the effect, an increase of the Seebeck coefficient is expected according to the Mott expression for the Seebeck coefficient:

$$S = \frac{\pi^2}{3} \frac{k_B}{q} k_B T \left(\frac{1}{n} \frac{dn(E)}{dE} + \frac{1}{\mu} \frac{d\mu(E)}{dE} \right)_{E=E_F} \tag{1}$$

where k_B is the Boltzmann constant, T is the temperature, $n(E)$ is the carrier density at energy E, $\mu(E)$ is the mobility at energy E, E_F is the Fermi energy, and q is the electronic charge.[40]

Doping with various carbon-based materials leads to improved TE performances due to different mechanisms, including energy filtering barrier formation. Based on this, the utilization of three components, that is, ternary systems,[41] is supposed to boost TE performance even further. In the work by Liu et al.[37] introduction of nanowires (NWs), in this case PEDOT NWs (PNWs) alongside SWCNTs into PEDOT:PSS matrix is reported. In the aforementioned work,[34] the influence of SWCNTs was investigated and led to a PF of ≈265 µW mK^{-2} at 60 wt% load with SWCNTs. In the present work, the influence of PNWs is investigated by keeping a fixed amount of CNTs. The increase of PNWs concentration in the system first leads to improved values of the Seebeck coefficient from ≈31 to 37.5 µV K^{-1} with further decay at higher CNT concentration. Such behavior is explained with the transition from a non-percolating to a percolating network, above a concentration corresponding to the percolation threshold for the investigated system., that is, the initial increase is due to the interfacial carrier EFM, which is negligible at higher concentrations due to the overwhelming presence of PNWs. The electrical conductivity shows slight decay with increased concentration of NWs. The optimal PF is equal to 352 µW mK^{-2} at the PNWs/PEDOT ratio 0.5 wt%. The change of Seebeck coefficient, which increased at higher NWs concentration and further decayed was explained with NW percolation threshold, that is, the interfacial carrier energy filtering (Figure 1d) that was influencing the thermopower became negligible at NW concentration above the percolation threshold. The current EFM could not be formed without the presence of both SWCNTs net and PNWs. Five-leg TEG formed from the manufactured samples showed high output power of 414 nW at $\Delta T = 40$ K; further 15-leg TEG showed output voltage of 5 mV. In addition to embedment in polymer matrix, C-based structures are also exploited for the fabrication of core–shell structures, which represent another way to improve the TE performance through fillers. Wang and co-workers[42] proposed the polymerization of EDOT monomers on the formed CNTs preliminary treated by sodium dodecyl sulfate, which enabled directionally preferable "growth" of polymer chains and created a core–shell structure (**Figure 2**a). The results revealed that increasing the CNT concentration led to a non-linear improvement of electrical conductivity (up ≈680 S cm^{-1}), associated to the strong interfacial interaction between π–π polymer chains and fillers, and the highly conducting 3D CNT network. Though the Seebeck coefficient is increasing as well with the increase of CNT concentration, authors do not give an explicit explanation of the mechanism behind the improvement of the property. The highest achieved
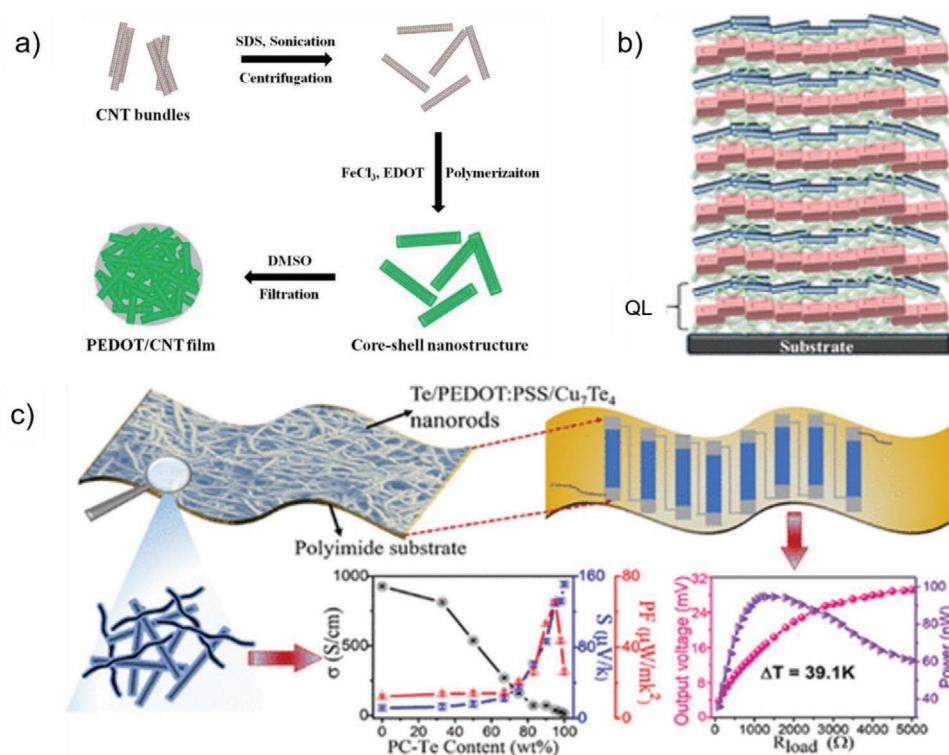
Figure 2. a) Formation and concept of core–shell structure. Reproduced with permission.[42] Copyright 2019, Elsevier Ltd. b) Sandwich-like structure or layer stacking where the quadruple layer (QL) structure is highlighted (QL composed of PDDA, PEDOT:PSS:graphene, PDDA, and PEDOT:PSS-DWNT). Reproduced with permission.[43] Copyright 2019, American Chemical Society. c) Formation of 3D network and its influence on TE output current. Reproduced with permission.[46] Copyright 2018, American Chemical Society.

PF is 157 µW mK^{-2} for 67 wt% concentration of CNT. Further treatment with PEI allowed switching the nature of the sample from p- to n-type with the decrease of electrical conductivity and Seebeck coefficient to 561 S cm^{-1} and −23 µV K^{-1}, respectively. Once both types of materials were obtained, the working TEG fabric was manufactured with output voltage ≈1.9 mV at ≈8 K temperature difference.

Both SWCNTs and MWCNTs are used as polymer fillers due to their good electronic transport properties or/and cheap and easy processing. For example, in the MWCNTs it is known that only two or three outer tubes are participating in electronic transport. Thus double-walled carbon nanotubes can be used for boosting up the TE performance of composite materials. In the work by Stevens et al.[43] the use of double-walled carbon nanotubes (DWCNTs) as filler within PEDOT:PSS matrix and further boost of TE properties via thermal degradation is reported. Authors created sandwich-like composites (Figure 2b) with layer by layer deposition, according to the following sequence: poly(diallyl dimethylammonium chloride) (PDDA), graphene/PEDOT:PSS, DWCNT/PEDOT:PSS. Incorporation of both DWCNTs and graphene into the matrix led to higher TE performance than that of individual layers. The configuration with four different materials (PDDA, PEDOT:PSS:graphene, PDDA, and PEDOT:PSS-DWNT) is marked as the quadruple layer (QL). Further heat treatment at 375 and 425 °C led to the degradation of the insulating parts (PSS and PDDA) of the stacked systems underlying carbon materials (fillers), resulting in more favorable electron transport through the composites.

The authors emphasized that no damage of fillers components was registered. The highest degradation point of PSS is reached at 375 °C resulting in PEDOT amount relative to PSS of 87 wt%. Transport properties tests showed that electrical conductivity slightly increases from 63.5 to 78 S cm^{-1} at 150 °C due to the water removal from the system; further treatment up to 300 °C diminished electrical conductivity, which is attributed to the presence of remnants from the decomposed parts of the system; the subsequent temperature treatment at 375 °C led to a significant increase of conductivity up to 170 S cm^{-1} and, finally, the treatment at 425 °C led to the highest value of 342 S cm^{-1} once the PDDA:PSS complex was almost completely degraded. However, the Seebeck coefficient exhibits improved values up to 79 µV K^{-1} at 375 °C treatment, with further decrease at higher temperatures. The decrease can be explained with an improved concentration of charge carriers, due to the removal of the insulating component of the system. Overall, the temperature treatment of the system led to an improved TE performance with increasing temperature, the highest PF of 168 µW mK^{-2} being reached at temperature of 425 °C. The increase of PF values can be also explained by an increase in carrier mobility via low contact resistance between graphene and nanotubes.[44] In parallel to CNTs, graphene is also used as a filler to boost the TE performance of the polymer matrixes due to its high transport properties. Liu et al.[45] showed that the incorporation of graphene at 2 wt% load into the PEDOT matrix led to a significant increase of electrical conductivity up to ≈1000 S cm^{-1} and an overall increase of PF up to 25 µW mK^{-2} at room temperature.

**ADVANCED
SCIENCE NEWS**

www.advancedsciencenews.com

**ADVANCED
FUNCTIONAL
MATERIALS**

www.afm-journal.de

No mechanism of TE performance improvement was, unfortunately, described.

According to the recent literature, CNTs attracted the most of attention, compared to other carbon-based materials, probably due to their peculiar morphological and electronic properties. The highest reported PF is ≈1200 µW mK^{-2}, which is an outstanding value for polymer-based systems. The high TE performance was achieved thanks to the outstanding transport properties of SWCNTs, which formed connected network, and the exploitation of the Soret effect. It was not mentioned, but it could be debated, if an EFM took place at the interface between nanotubes and polymer. Overall, the reported results are encouraging, even if the lack of data on thermal conductivity for most of the works, makes it difficult to elucidate how the actual efficiency was obtained.

2.2. Organic/Inorganic Composites

Apart from carbon-based materials, a variety of inorganic materials are also used as fillers for polymer-based composites. Their application is due to their unique transport properties at the nanoscale and the technical advantages of composite manufacturing, when superior properties of different materials can be synergistically combined in the final composite.

Cu$_7$Te$_4$ Nanorods: As an instance, Lu et al.[46] used simultaneously two different fillers, that is, Te nanorods, and Cu$_7$Te$_4$ nanorods, respectively. By the introduction of the two fillers, the formation of the nanorod-based 3D network was achieved (Figure 2c). With the increase of Te content, the decrease of electrical conductivity was observed, whereas the Seebeck coefficient kept increasing due to the increased mobility and decreased concentration of charge carriers, respectively. The growth of S was also due to the interfacial energy filter between nanorods and polymer matrix, which allowed scattering low-energy charge carriers.[47] The highest PF for such a system is ≈65 µW mK^{-2} for 95 wt% PC-Te at 300 K, which gives the high figure-of-merit ZT = 0.1 thanks to the low thermal conductivity (0.2 W mK^{-1}). The mechanical test of output voltage under stretching showed a stable behavior with a maximum power density of 39 µW cm^{-2} and 39 K temperature gradient.

SnSe Nanosheets: If Te doping is applied to an SnSe system, even higher TE performance can be achieved as shown in the work by Ju et al.[48] Te-doped SnSe nanosheets (NSs) were covered by polymerized EDOT monomers. With the increase of PEDOT concentration in such NSs the decrease of S and increase of conductivity were observed due to higher contribution from conductive PEDOT and lowered contribution from NSs. However, the more rapid growth of σ overwhelmed the reduction of S, resulting in an overall enhancement of TE PF of the system up to ≈145 µW mK^{-2}. The material was further used to obtain a layered structure with pure polymer in alternating layers (AL). With the increase of AL layers, the decrease in volume content of the matrix and the increase of electrical conductivity were observed, which is counterintuitive. Such unexpected behavior was explained with increased interaction between stretched/arrayed chains of spin-coated matrix and clustered chains within the composite, resulting in improved charge hopping mechanism of conductivity. The

charge hopping mechanisms occurs through the vertical layers of different materials (**Figure 3**a). This stacked configuration of the layers is a promising approach in boosting the TE performance. The highest PF (≈220 µW mK^{-2}) was achieved for a composite system with three AL layers. Nanostructures of Te can be used as depositing material. In the work by Ni et al.[49] the manufacturing of layered hybrid structure is reported. PEDOT NWs were used as a working electrode with further electrodeposition of Te around the matrix in presence of 0.1 M H$_2$SO$_4$. The process took 7 h resulting in the decrease of electrical conductivity (compared to pure PEDOT NWs) from 1340 to ≈560 S cm^{-1} and in the growth of the Seebeck coefficient from ≈15 to ≈65 µV K^{-1}. The PF after the deposition is eight times higher (up to ≈240 µW mK^{-2}) than for samples before deposition (≈30 µW mK^{-2}). The increase of TE performance is due to the synergetic effect of the combined use of organic and inorganic materials.

Bi$_2$Te$_3$ Nanowires: The use of inorganic systems as fillers is accompanied by the risk of the presence of a high energy barrier between interfaces. This problem was precisely addressed by Kim and co-workers, by modulating[52] the energy barrier between polymer matrix and Bi$_2$Te$_3$ NWs. This was achieved through the use of polar solvent vapor during annealing, that is, the composite materials were treated with the DMSO vapor in a closed chamber at 80 °C. Energy barrier at the interface is defined as the difference between the work functions of Bi$_2$Te$_3$ and PEDOT: PSS. The Seebeck coefficient increases from 36 up to 45 µV K^{-1} with the change of energy barrier from negative (–0.1 eV) to positive (0.11 eV) through the increased treatment time. Surprisingly, the electrical conductivity increases almost linearly from ≈620 to ≈1000 S cm^{-1} with treatment time and achieves its maximum after 120 min. The simultaneous increase is attributed to the filtering effect, allowing only to high energy charge carriers to pass through and thus increasing the mobility, along the removal of the PSS insulating part from the system. The highest achieved PF for the samples was 205 µW mK^{-2} at 120 min of PSVA treatment and interface energy barrier ΔE = 0.11 eV.

Ge Thin Film: Another way to optimize the TE performance is to modify the interface of a composite by the deposition of a thin film. Lee et al.[50] studied the deposition of undoped Ge thin film. The application of Ge leads to the shift of energy levels at interface for both materials, that is, modulation doping or Kraut's method, which is shown in Figure 3b. The shift of energy levels artificially created a valence band offset (VBO), the advantage of which is an improvement of the overall mobility of charge carriers without changing their concentration. As a result, an increase of the Seebeck coefficient (≈398 µV K^{-1}) was observed due to the induced hole transfer from polymer to Ge and charge carrier's concentration gradient. The highest achieved PF is 154 µW mK^{-2}.

In most of the cases, the research focuses on the implementation of metal-based inorganic materials in polymers, but a variety of other materials have also been tested. For example, the implementation of oxides or elements such as black phosphorus (BP),[53] which led to the simultaneous improvement of both electrical conductivity and Seebeck coefficient. Improvement of electrical conductivity (up to 1446 S cm^{-1}) is explained by an increase of hole mobility due to the reduced
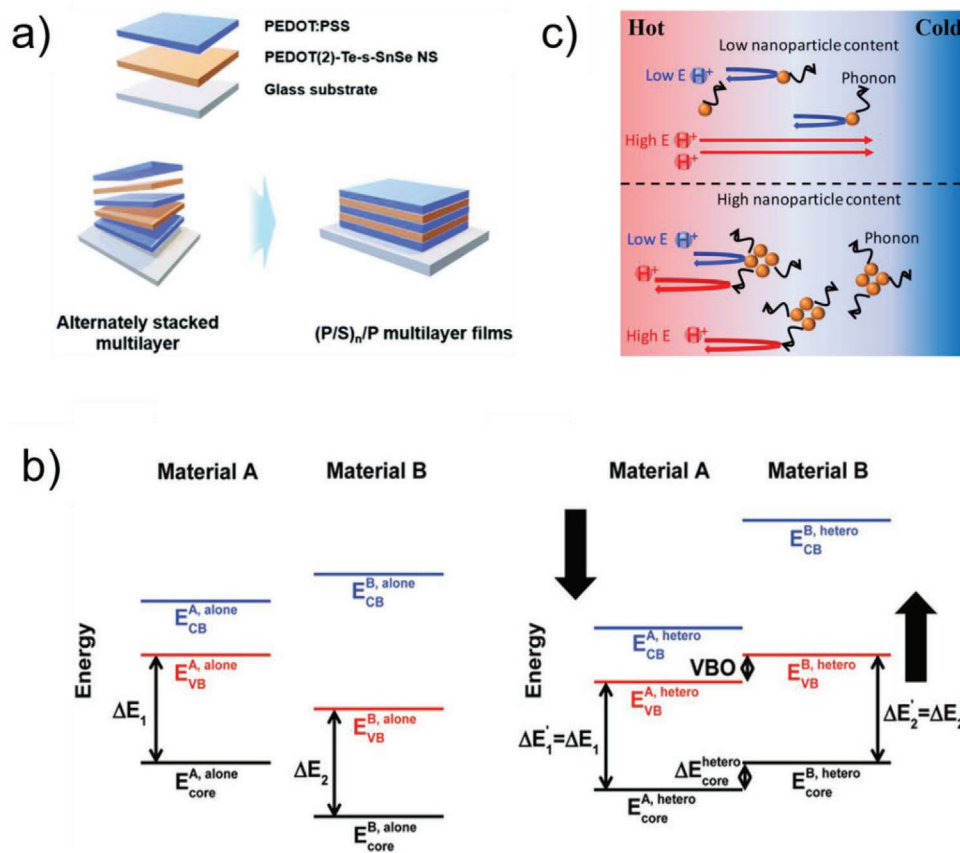
Figure 3. a) The layers of polymer/SnSe nanosheets and through the layers increased charge-hopping. Reproduced with permission.[48] Copyright 2019, Royal Society of Chemistry. b) Kraut's method for Ge application, Reproduced with permission.[50] Copyright 2018, WILEY-VCH. c) Schematic representation of hole-phonon scattering. Reproduced with permission.[51] Copyright 2019, Elsevier Ltd.

electron-phonon coupling.[54] The increase of the Seebeck coefficient is due to the intrinsic high values of that parameter for BP. The filtering of charge carriers is the main mechanism operating in the composite. As a result, the highest PF (36 μW mK^{-2}) is achieved for sample with 2 wt% of BP and represents 109% increase over pure polymer. Though the PF does not exceed 40 μW mK^{-2}, unlike other published research, where concentration exceeded 50%, the highest concentration is only 2 wt%, which is a remarkably small amount for such improvement in performance. Though the achieved result is not among the highest in the field, such approach can be further used as a secondary doping agent to further boost preliminarily enhanced transport properties.

Te Quantum Dots: The inorganic filler is usually used in the form of spheres or rods, for further creation of a core–shell structure, where the polymer (shell) covers the filler (core). Unfortunately, such systems and their syntheses suffer problems: inhomogeneity, large particle size, ineffective loading, and so forth. A way was demonstrated[55] to obtain synchronized production of PEDOT:dodecylbenzensulfonate and Te quantum dots, which resulted in highly homogeneous material. The increase of electrical conductivity (up to $\approx$1400 S cm^{-1}) is explained with the improved variable range hopping conduction due to the delocalization of carriers with improved structural order[56] Additionally, the increase of Te concentration

results in lower carrier concentration, and, as a result, in higher mobility, thus in the increase of the Seebeck coefficient. The degradation of the functional properties occurs with the increase of the size of Te quantum dots above 5 nm, which is explained by improved phonon scattering below the phonon frequency. According to the calculation, the size of dots should not exceed 2 nm at room temperature for successful improvement of Seebeck coefficient.

Among inorganic-based systems for the creation of hybrid composites, researchers are not infrequently using conventional semiconductor systems. The core (polymer) and shell (Bi_2Te_3 nanowire) structure[57] was formed via in-situ one-pot synthesis, based on which a scalable 3D network of self-assembled nanofilms incorporated with hybrid nanowires was created with elevated TE performance for highly porous material-foam. The addition of sodium dodecyl sulfide and ethylene glycol allowed reaching high output power (up to 130 μW) at low temperature (less than 100 °C) with unprecedented 15 days stability.

Cu_XSe_Y Nanowire: Overall, the utilization of wire-type structures is very promising due to the alignment of the wires and anisotropic properties, with preferential directionality. As an example, the in-situ synthesis of Cu_XSe_Y NW within the polymer matrix is obtained.[58] The system was further cold pressed on the bendable substrate to improve the contact between NWs and matrix. The highest PF ($\approx$390 μW mK^{-2})

**ADVANCED
SCIENCE NEWS**

www.advancedsciencenews.com

**ADVANCED
FUNCTIONAL
MATERIALS**

www.afm-journal.de

was achieved for the Cu/Se nominal molar ratio of 3 at elevated temperature ≈420 K. Improved Seebeck coefficient is related to the natural high S of the CuSe filler. Increase of temperature changes the behavior of the system, due to a α- to β-phase transition of NW and the shift of the Fermi level.

$Cu_{12}Sb_4S_{13}$ Nanoparticles: As thermoelectricity is seen as an environmentally friendly energy source, emphasis has been given to the development of efficient TE systems based on earth-abundant elements or composites, aiming at obtaining high functionalities through the use of a "green" approach. In this respect, the incorporation of $Cu_{12}Sb_4S_{13}$ nanoparticles into polymer nanofibers was demonstrated, with the improvement of electronic transport properties at only 5 wt% filler concentration.[51] The surface of the nanoparticles was modified by ligand, via salt treatment ($SbCl_3$, $InCl_3$, NH_4SCN). During the process, oleylamine (OLA) was formed on the surface of nanoparticles. A simultaneous increase of both the electrical conductivity and the Seebeck coefficient was obtained for the nanoparticles covered with $SbCl_3$. The positive changes of properties are explained with the energy scattering by the low energy barrier and hole-phonon scattering (see Figure 3c), which was achieved due to the alignment of energy levels between filler and polymer. Further increase of concentration led to decrease of Seebeck coefficient due to the improved hole-phonon scattering, which diminished the contribution from the high energy charge carriers. The resulting ZT of the bulk composites is 2.5 times higher (0.01) than that of previously reported PEDOT nanofibers.

Alongside incorporation of inorganic systems, creation of different structures is another way of tuning TE performance of polymers.[59] The increase of Seebeck coefficient up to 120 $\mu V\ K^{-1}$ at 150 °C for polymer matrix via sandwich-like structures with aluminum and gold resulted in creation of various interfaces between metals and polymer. The increase of S at increased temperature, when different metals are used, is explained by the polarization of the surface due to electron-phonon coupling, since the semi-metallic polymer matrix possesses high amount of polaron energy levels in bandgap. The increase of S led to a negligible decrease of the electrical conductivity, resulting in PF value of 96 $\mu W\ mK^{-2}$ at a temperature difference of 8 °C.

Among the reported works, those that used conventional semiconductor-based systems in a nanosized form, despite the achieved improvements, they have not shown breakthrough results or even exceeded the functionality exhibited by systems, where organic fillers were used. It seems that utilization of inorganic systems is not as promising as other approaches at least in the state-of-the-art TE composites.

2.3. Chemically Modified Composites

Incorporation of different (either organic or inorganic) fillers is indeed a highly effective strategy to improve the TE performance of the polymers due to high reproducibility of results. However, certain restrictions exist for this method, such as concentration limits, agglomeration, incompatibility of the resulting electronic band structures and others. For this reason, chemical treatment of polymers, with/without addition of fillers, represents, per se, a good alternative to improve the TE properties of polymer-based materials. The latter can be neglected via chemical treatment. Moreover, the chemical treatment of the polymer matrix itself is able to induce an adjustment of the electronic band structure and changes in energy levels, the shift being dependent on the applied chemicals, thus making this strategy very promising.

Among different chemicals, ionic liquids (IL), which are particles carrying charge (stable ions) in a liquid form, were used[60] for surface treatment of polymers, leading to an improvement of the Seebeck coefficient, ultrahigh values of PF without significant effect on electrical conductivity. Three ILs (1-ethyl-3-methylimidazolium tetrafluoroborate (EMIM-BF4), 1-ethyl-3-methylimidazolium bis(trifluoromethylsulfonyl)imide (EMIM-TFSI) and 1-ethyl-3-methylimidazolium dicyanamide (EMIM-DCA) were used to create heterostructures (see the scheme in **Figure 4**a), in which ILs are preliminary treated with acids and bases polymer matrix.[61] The final samples exhibit form of thin polymer films covered with liquid/gel-like transparent layer. The highest values of electrical conductivity and Seebeck coefficient, ≈1600 S cm^{-1} and 65 $\mu V\ K^{-1}$, respectively, were achieved with EMIM-DCA treatment giving a final PF of ≈750 $\mu W\ mK^{-2}$ at 30 vol%. Improved S and σ are obtained through the Soret effect[62] and the samples demonstrate insensitive to relative humidity and ion migration due to their peculiar structure, in which polymer surface is isolated with ILs from a water in the surrounding media.

Thermodiffusion or Soret effect is a phenomenon that can be observed in materials with porous structure and presence of liquid. The phenomenon describes different response of ions to the force induced by a temperature gradient. The effect can be considered as a microscale effect.[63–65] The mean free path of the particles is inversely correlated with their size, the smaller the particles are the longer distance they can travel. The effect is considered positive when particles move from hot to cold side, and negative at the reverse flow.

According to author's interpretation the described Soret effect leads to the generation of an electric field throughout the whole sample after accumulation of ions in the cold part of the material.[60] According to the authors, the built in electric field scatters low energy holes or raises the hole energy. To our opinion, the formation of the macroscopic electric field seems being rather unlikely and this point is debatable. Indeed, due to the porosity of the samples, ion motion through the whole sample could be inhibited. It is more believable that the Soret effect is indeed taking place within the samples, but the contribution is different from what is stated by the authors. The contribution is likely to be in providing additional charge carriers (moving ions) thus increasing overall charge carrier concentration. Either way, the mean energy of the holes increases, which causes an increase of the Seebeck coefficient. The mechanism is similar to the energy-filtering effect. The highest ZT of the reported results is 0.75, which is even more impressive considering the high stability of the system in air.

Similar behavior was described in the work by Guan et al,[66] where acid-treated PEDOT:PSS (A-PP) was covered with polyelectrolytes, poly(4-styrenesulfonate acid) (PSSH) or poly(sodium 4-steresulfonate) (PSSNa). It was found that the obtained heterostructure system exhibits higher Seebeck coefficient but
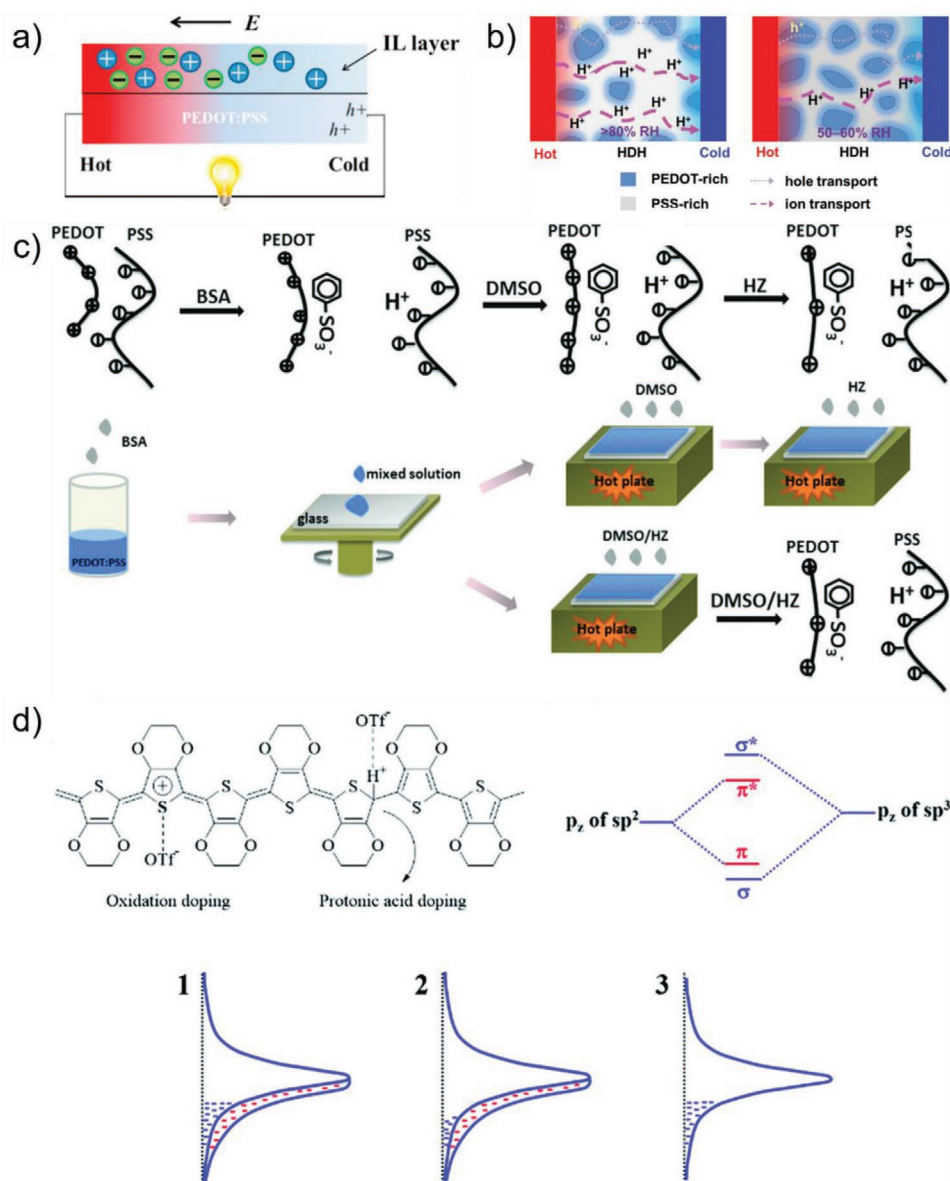
Figure 4. a) Formation of heterostructure of ionic liquid above the polymer layer, Reproduced with permission.[60] Copyright 2018, Elsevier Ltd. b) Enhanced thermal migration of H+ through polymer via increase presence of PSS and water. Reproduced with permission.[68] Copyright 2018, WILEY-VCH. c) Phase separation within sample via DMSO treatment. Reproduced with permission.[69] Copyright 2018, WILEY-VCH. d) Scheme of oxidation and proton doping with formation of π–π^* orbitals with reflectance in DOS 1) synthesized, 2) dedoping via reducing agent 3) de-doping by NaOH. Reproduced with permission.[70] Copyright 2018, Royal Society of Chemistry.

lower electrical conductivity values. The mechanism behind this behavior is the Soret effect, that is, in this case the protons of polyelectrolyte and holes of A-PP are accumulated on the cold side of the material. The accumulated protons in the polyelectrolyte layer creates the barrier for hole transport in the A-PP layer hence the filtering effect is taking place. Decreased charge density of the system lead to the improved entropy. Summarizing the Soret effect presence (diffuse and accumulation of ions) enables energy filtering effect. The described study by Guan et al.[66] supports the work by Fan et al[60] and provides descent explanation. Once the relative humidity (RH) is increasing the Seebeck values keep growing and electrical

conductivity keeps decaying. Final achieved power factor of the system is 401 µW mK^{-2}.

Inspired by that work, Saxena et al.[67] described the use of ILs 1-ethyl-3- methyl imidazolium dicyanamide, (EMIM DCA), 1-ethyl-3-methyl imidazolium tetracyanoborate (EMIM TCB) and 1-ethyl-3-methyl imidazolium tetrafluoroborate (EMIM BF4) as post-treatment agents for tuning the TE properties. Here no preliminary step was applied to treat polymer with acids and bases, which makes the process simpler. Despite its simplicity, a drawback is present: the lack of acid/base treatments makes the electrical conductivity less sensitive to ILs treatment. Though the effect of ILs treatment on electrical

**ADVANCED
SCIENCE NEWS**
www.advancedsciencenews.com

**ADVANCED
FUNCTIONAL
MATERIALS**
www.afm-journal.de

conductivity is smaller, it is visible unlike the previous study.[61] The increase of the Seebeck coefficient ($\approx$42 µV K^{-1}) as well as of the electrical conductivity ($\approx$900 S cm^{-1}) were observed. The latter is well explained by the shift of bipolaronic to polaronic states (proven by UV–vis) and ability of IL to remove the PSS part, whereas the driving force for the growth of S is only suggested. Authors address the molecular properties of the used anions, hence the DCA anion with strongly localized charge shows the highest basicity, resulting in the strongest (among other anions) interaction with PEDOT. For the studied systems, the highest PF of 170 µW mK^{-2} was achieved for the EMIM DCA post-treated sample.

Ionic contribution can play a crucial role in determining the TE properties. The presence of H$^+$ cations within the system can boost TE performance. However, it is relevant only at high humidity conditions. In the work by Kim et al.,[68] the influence of different PEDOT:PSS ratios was studied; the presence of PSS typically leads to low electrical conductivity. In the present work, instead, an excess of PSS can be used to enhance the Seebeck coefficient of the system via incorporation of H$^+$ within the system at high humidity of the surrounding environment (see the schematic representation in Figure 4b). The use of PEDOT with the highest PSS ratio (1:6) with poly(styrene sulfonic acid) (PSSH) treatment allows improving Seebeck coefficient up to $\approx$10 mV K^{-1}, which is 1000 times higher than that of pure PEDOT:PSS. Further increase of humidity up to 90% results in even higher value of S, $\approx$16 mV K^{-1}. Electrical conductivity of such system is much lower ($\approx$29 S m^{-1}) compared to pure polymer matrix. The tremendous increase of the values of Seebeck coefficient is explained with improved presence of the PSS part due to PSSH treatment. PSS localization allows improving ionic contribution to the S values. Incorporation of H cations tends to further increase the values, creating double (PSS and H) ion flow through the system. High humidity plays a second important role, by allowing the polymer matrix to absorb water from the environment, thus easing the flow of ions. However, such systems need high and constant HR level to be operational. For that purpose, the films were covered with the hybrid inorganic/organic system (Zr$_6$O$_4$(OH)$_4$(-COO)$_{12}$/Hydrogel) allowing constant access of moisture to the system. The resulting PF and thermal voltage are 7.8 mW mK^{-2} and 81 mV, respectively, at 5 °C temperature difference.

Not only pure materials can be used for chemical treatments but also the combination of agents. The influence of stoichiometry of IL mixtures (1-ethyl-3-methylimidzole/chloride, 1-ethyl-3-methylimidzole: bis(trifluorosulfonimide), 1-methylimidazole, HTFSI)[71] on the TE properties was tested. Unlike the previous reports, the IL mixtures were used as additives, which affected the viscosity of the polymer at the liquid phase and restrained the possible maximum of the IL volume that can be added to the system. The addition of IL mixtures with a 1:1 ratio showed a significant increase of electrical conductivity (from 6 to 1000 S cm^{-1}) due to the favorable morphological rearrangement and improved the continuity between polymer domains. However, the Seebeck coefficient shows no change in values, due to the absence of ion-exchange of IL with the polymer matrix. Changing the stoichiometry to 4:1 did not change the behavior of electrical conductivity from 1:1 ratio due to higher viscosity, but it affected the behavior of the Seebeck coefficient, which

increased with the rise of volume percentage of the additive in film. A double increase of S is explained with cations of IL to be associated with PSS part of polymer rather than with their own counter ions. Overall, the additive with more diffusive cations is more capable of the ion-exchange process with the polymer matrix and the increase of S is driven by a shift of charge carrier population from bipolarons toward polarons. In this work, the chemical agents were applied during the process of film preparation, whereas other strategies emphasize the importance of polymer treatment during and after the preparation of polymer films. In the work by Wang et al.,[69] it is shown that the addition of benzenesulfonic acid into polymer solution tends to increase the transport properties, which results in improvement of electrical conductivity (up to $\approx$2000 S cm^{-1}). Improvement of electrical conductivity is explained by the spatial structure, that is, the bulkier functional groups are, the lower increase of electrical conductivity is observed. The treatment with acids led to the promotion of polaron formation and to the improvement of the charge carrier's mobility through chain. Further adjustment of the oxidation level via the dedoping process with DMSO and hydrazine increased the Seebeck coefficient and resulted in PF of $\approx$200 µW mK^{-2}. The increase of S is explained with the formation of peaks associated with the conversion from bipolaron to polaron states in absorption spectra, which reflects in phase separation (Figure 4c) of PEDOT$^+$ and PSS$^-$. The TE generator based on these samples allowed to reach thermovoltage of 4.6 mV at 8 °C temperature difference.

The counter ion in the polymer plays a crucial role for stability and transport properties. Thus, it should be carefully considered for TE application. In the work by Yao et al.[70] the change of conventional PSS part to trifluoromethanesulfonate (OTf) is reported, with further NaOH post-treatment. The intrinsic TE properties of polymerized PEDOT:OTf films are $\approx$3300 S cm^{-1} for σ and 32 µV K^{-1} for S, respectively, which resulted in a PF of $\approx$350 µW mK^{-2}. Post-treatment process allows improving the Seebeck coefficient ($\approx$51 µV K^{-1}) with a slight decrease of electrical conductivity ($\approx$2300 S cm^{-1}), which resulted in an overall increase of PF up to $\approx$570 µW mK^{-2}. Changes of both properties are due to the dedoping process (Figure 4d) by NaOH. It is estimated that post-treatment led to a lower concentration of OTf$^-$ anions and that dedoping is driven by protonic acid doping. XPS of the post-treated film showed a shift of the C-S XPS band due to the removal of protons from the PEDOT part of the polymer. Additional tests showed that all the samples hold excellent stability under ambient conditions. The chemical treatment of the polymer matrix can be processed at various conditions. In the work by Myint et al.[72] the polymer composition was adjusted via chemical treatment with HNO$_3$ followed by fluxing nitrogen gas with external pressure 0.2 MPa. A synergetic positive effect was demonstrated from both chemical treatment and pressure tuning during treatment, that is, HNO$_3$ led to protonation of the PSS part, which resulted in phase segregation between the insulating (PSS) and the conducting (PEDOT) parts of polymer, alongside the conformation of polymer chains, which improved the mobility of charge carriers, hence the increase of electrical conductivity (up to $\approx$2700 S cm^{-1}). The treatment changed the temperature behavior of the films from semiconducting to metallic or semi-metallic, at which

electrical conductivity decreases, while the Seebeck coefficient decreases with temperature growth. The maximum PF of the work is ≈95 µW mK^{-2} at 150 °C.

As already mentioned, tuning the TE properties through oxidation/reduction processes is of high interest to skip polymerization steps and to focus on the adjustment of the functionality of the products. Li et al.[73] tuned the TE performance of the matrix via polyethylenimine ethoxylated (PEIE) solution mixed with EG and further H_2SO_4 treatments. Both treatments led to the aggregation of PEDOT chains due to the interaction between cations and PEIE, and rougher surface of the matrix due to the phase separation with PSS/PEIE parts, respectively, resulting in the crystallization of PEDOT molecules. During the chemical treatments, the polymer matrix endured a decrease of π–π stacking and lamellar spacing distances, resulting in the formation of a PEDOT nanocrystal film. Overall, PEIE/EG dipping led to the reduction, whereas H_2SO_4 to the oxidation of the film, which increased the ratio between N (neutral amine) and N$^+$ (protonated amine of PEIE), leading to higher values of the Seebeck coefficient (≈25 µV K^{-1}) and of the electrical conductivity up to ≈3770 S cm^{-1}. In addition, such a drastic increase can be explained by the formation of PEIE:H_2SO_4 stacks with further removal and decrease in thickness of nanofilms. The optimal PF and ZT of the systems are 133 µW mK^{-2} and 0.019, respectively. Although the proposed methodology exhibits some advantages, like, for instance, very high electrical conductivity, comparable and even higher than some reported inorganic-based materials (for example, BiCuSeO, SnSe, and SiGe), an intrinsic drawback is that the properties of the matrix risk to be modified and worsened during the synthesis. In another attempt to modify the TE functionality through chemical treatment, polymer NWs were produced via a modified self-assembled micellar soft-template approach, by varying the growth time, followed by sulfuric acid and NaOH post-treatment,[74] resulting in 1D PEDOT films made of polymer NW. Initial transport properties for the samples are ≈1340 S cm^{-1} and 15 µV K^{-1}. UV–vis results showed that acid treatment led to bipolaron state enhancement, resulting in higher doping level and σ up to ≈1720 S cm^{-1}. However, further base treatment led to de-doping process and doping type changes from bipolaron to polaron and even neutral states, with increase of S up to 25.5 µV K^{-1} and decrease of σ down to ≈715 S cm^{-1}. The described influence which led the improvement of the TE performance is different from the conventional one, where sulfuric acid treatment leads to PSS removal, decrease of thickness, and uneven height of the samples. The achieved PF of ≈46.5 µW mK^{-2} is the highest reported so far among 1D PEDOT-based materials.

The Soret effect seems the most effective strategy and proved to be the most efficient, reaching PF of mW mK^{-2} instead of µW mK^{-2}, which is usually a case. The uniqueness of the work[73] is in usage of known disadvantage, which is a presence of insulating PSS, in a building of a new approach turning it into an advantageous system with increased PSS presence. A utilization of the Soret effect is even more efficient once the polymer is preliminary treated with acid/base substances leading to phase separation and higher influence of ILs, which was clear from the comparison of the works by Fan[60] and Saxena.[67]

3. P3HT

Poly(3-hexylthiophene) (P3HT) is widely used in organic electronics. Its vast application is dictated by a number of factors, such as its semiconductor nature, its intrinsic electrical conductivity, and its good solubility. The performance of materials based on polymer matrixes is sensitive to the quality of the material, that is, the regioregularity, which affects the electronic properties and further possible adjustments via physical, mechanical, or chemical interactions. The application of P3Ht as TE material is interesting because of its high intrinsic thermopower, especially compared with PEDOT:PSS, which exhibits values orders of magnitude lower. However, the intrinsic electrical conductivity in P3HT is quite low and the main challenge is to increase σ, without affecting S, to obtain a high power factor.

3.1. Use of Carbon-Based Materials

P3HT is one of the most studied conductive polymers for TE application, but only two research works have been recently published, where carbon-based fillers were used alongside this matrix. As it happens in both the works, SWCNTs were used as filler content. However, the achieved results are not similar. Tonga et al.[75] report that the P3HT's TE performance can be tuned up by iodine-crystal-air-treatment, that is, iodine crystal in a closed vial reacts with the polymer matrix via air medium. The high value of PF up to ≈148 µW mK^{-2} was dependent on P3HT type (regio-regular/random), the concentration of filler, and finally the solvents used during the process. For example, iodine treatment improved the electrical conductivity for solvents with a lower boiling point like $CHCl_3$ and CCl_4. Regioregular (RR-) matrix gives an increase of electrical conductivity by an order of magnitude compared to regiorandom (RA-) one. This behavior for different matrixes is explained by higher intrachain planarity and better interchain packing for RR-P3HT. Incorporation of carbon nanotubes (up to 50 wt%) in combination with the iodine treatment led to up to 800-fold increase of conductivity, resulting in values up to 1722 S cm^{-1}. The presence of SWCNT decreased S by 30% (≈28 µV K^{-1}) at the highest load of filler. Further research works in the case of iodine doping in air requires encapsulation of the sample's surface.

Kang and co-workers[76] report a more conventional processes by mixing CNTs with polymer, by using small-bundled carbon nanotubes (SSWCNTs), that is, the connected stacks of nanotubes. The filler was incorporated via micronizing mill into two different polymers: P3HT and poly(diketopyrrolopyrelle-selenophene) (PDPPSe) within dichlorobenzene as a solution. The increase of performance for both the composite systems is explained by the formation of the SSWCNT network and improved charge transfer through efficient hopping or tunneling mechanism (**Figure 5**a). Interestingly, the electrical conductivity for PDPPSe was higher (≈530 S cm^{-1}) than for P3HT (≈130 S cm^{-1}), due to the planar molecular structure (for PDPPSe), leading to extended delocalization of π-electrons, and orientation of the conjugated polymer, leading to a reduction of the inner-distance between PDPPSe and SSWCNTs due to mutual attraction. Negligible decrease of S, when the electrical conductivity increases rapidly is not trivial, due to the conventionally mutual exclusive relation between these
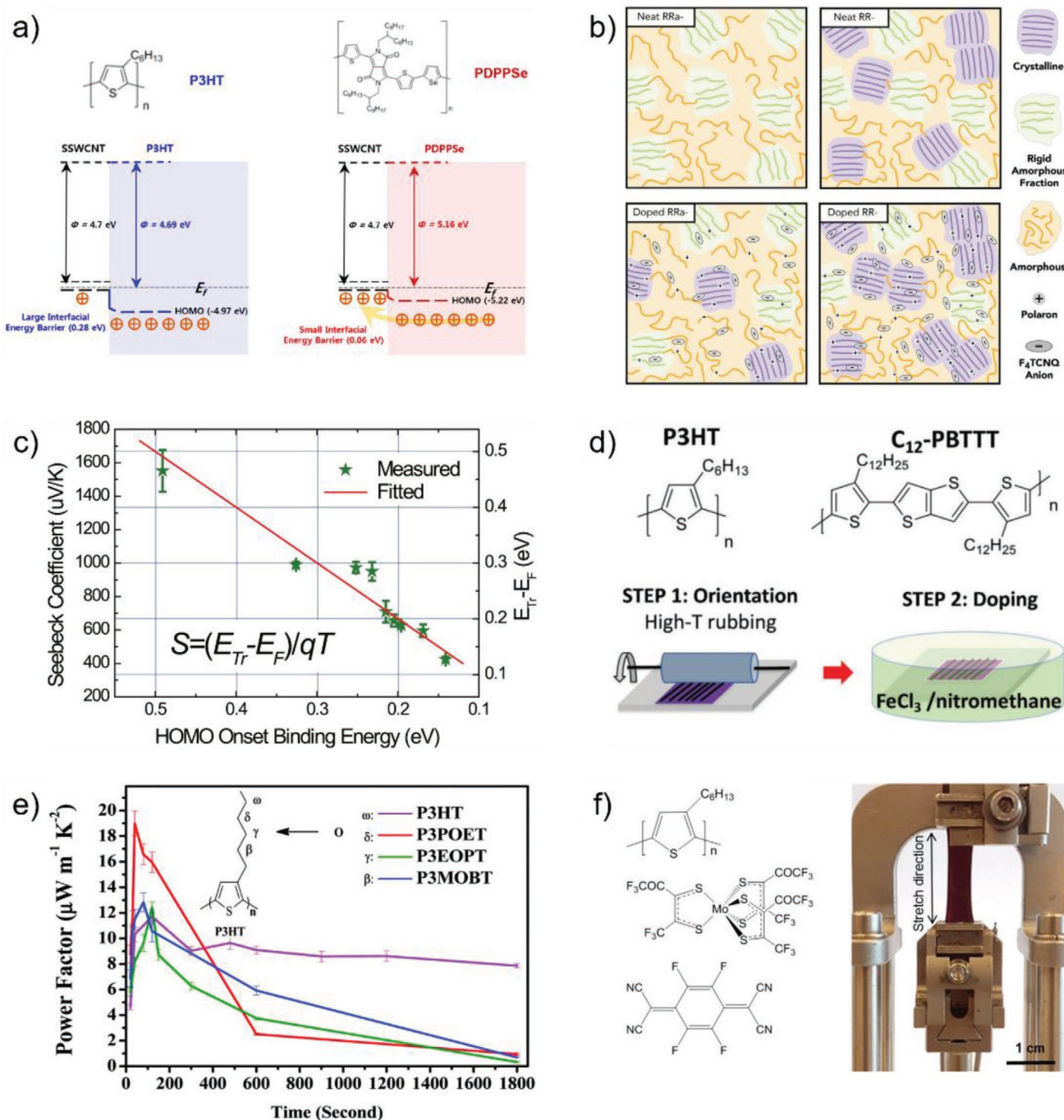
Figure 5. a) Filtering mechanism alongside tunneling via enhanced concentration of SWCNTs, Reproduced with permission.[76] Copyright 2019, American Chemical Society. b) Scheme of ordering of the polymer structure, Reproduced with permission.[81] Copyright 2019, WILEY-VCH. c) Influence of HOMO edge change on electronic structure and thus Seebeck coefficient, Reproduced with permission.[82] Copyright 2018, Elsevier Ltd. d) Orientation of polymer via rubbing, Reproduced with permission.[83] Copyright 2019, WILEY-VCH. e) Change of structure via incorporation of oxygen into backbone of polymer, Reproduced with permission.[22] Copyright 2019, Royal Society of Chemistry. f) On the left, chemical structures of P3HT, Mo(tfd-COCF₃)₃, and F4TCNQ; on the right, a stretching of polymer sample. Reproduced with permission.[84] Copyright 2019, American Chemical Society.

two properties. Such behavior is explained by the difference in interfacial energy barriers (0.06 and 0.28 eV) for PDPPSe and P3HT, respectively. Low energy barrier at the interface results in filtering mechanism determining that only (major) high energy charge carriers can pass through, which is reflected in higher

S values for PDPPSe-based composites. The highest PF values for PDPPSe and P3HT-based samples are 210 and ≈20 μW mK⁻², respectively. The TEG based on the composites showed an output power of 0.35 μW for PDPPSe/SWCNTs, which is five times higher than that of P3HT/SWCNTs (≈0.07 μW).

**ADVANCED
SCIENCE NEWS**

www.advancedsciencenews.com

**ADVANCED
FUNCTIONAL
MATERIALS**

www.afm-journal.de

3.2. Organic/Inorganic Composites

Sb₂Te₃: Besides the utilization of P3HT as an alternative TE material, it is also used as a binding "glue" for conventional semiconductors. Jang et al.[77] reported on 2,3,5,6-tetrafluoro-7,7,8,8-tetracyaniquinodimethane (F4TCNQ) doping with different concentrations (17, 25, and 33 wt%). Values of electrical conductivity and Seebeck coefficient up to ≈1.8 S cm⁻¹ (seven orders of magnitude improvement) and down to 100 µV K⁻¹, respectively, resulted in the PF of 1.6 µW mK⁻². Unlike standard literature, where the TE properties are summarized as an output voltage of the TE generators, the current study used the new materials as a binding agent or a glue for Sb₂Te₃ particles and compared the obtained TE properties with an epoxy binder. Unfortunately, TE performance of obtained Sb₂Te₃/P3HT composites did not surpass the one of epoxy-based, which is explained with more tightly packed particles for an epoxy system, resulting in higher electrical conductivity. The most original part of the study is in the application of the obtained composites, that is, the utilization of the polymer as a "glue" for other materials. Such application is debatable especially due to its lower TE performance, compared to epoxy-samples. However, the chosen route, if properly adjusted, can create additional energy barriers within composite materials, thus boosting the TE properties via EFM.

PbS Quantum Dot—MoO₃: The polymer matrix can be used in a sandwich-like structure with additional adjustment of the polymer structure itself alongside the surface. Sun et al.[78] reported the incorporation of PbS quantum dots into the P3HT matrix with further use of a MoO₃ interlayer. Doping of the matrix with quantum dots led to improved crystallinity and a slight decrease of bandgap from 2.07 eV down to 2.05, 2.04, and 2.03 eV at dots:matrix ratios 1:8, 1:4, and 1:2, respectively. However, the presence of quantum dots leads to a decrease of Seebeck coefficient values in the temperature range from 25 to 100 °C, which is due to the increased carrier concentration: the higher the concentration of dots, the higher the charge carrier concentration is. The same reason is behind the increase of electrical conductivity from 0. 012 S cm⁻¹ for pure polymer to 0.036 S cm⁻¹ for 1:2 doped matrix. However, once the temperature increases, the electrical conductivity tends to decrease due to the scattering effect of electrons and phonons. Further application of interlayer led to quite strong change of transport properties. The presence of the MoO₃ interlayer led to the increase of Seebeck coefficient by about 30% at the whole temperature range without affecting the trend. The positive trend for electrical conductivity with temperature increase is attributed to the polarization of the MoO₃ layer, which is increased at higher temperature. Overall, the polarization difference along the vertical direction of the device alongside the entropy difference contribute to the improvement of potential of the device resulting in six times increase of device's PF.

3.3. Chemically Modified Composites

Doping via chemical species is a common technique to improve the TE performance of polymer matrixes; however, during doping, both the short- and long-range order of the matrix can undergo changes and it is important to investigate the influence of doping on the crystallinity of the matrix. Hyhynen et al.[79] studied the influence of the crystalline order on the Seebeck coefficient of P3HT composites doped with (F4TCNQ) from the vapor phase. To change the crystallinity order various solvents (chloroform, chlorobenzene, toluene, p-xylene, etc.) alongside 3 min exposure of samples to F4TCNQ were applied. The exposure or doping led to 10 times improvement of charge carrier's mobility from 0.05 to 0.5 cm² V⁻¹ s⁻¹. The most disordered system (chloroform treated) exhibits *S* equal to 51 mV K⁻¹; further increase of the crystalline order increases *S* (up to 60 µV K⁻¹). However, the most ordered system (treated with p-xylene) shows only 43 µV K⁻¹. Based on an accurate analysis of the present literature in the field, it was concluded that the increase of *S* is due to the improved charge carrier's mobility thanks to the presence of ordered domains. Further decrease of *S* (occurring for the most ordered sample) is due to the sudden increase of charge carrier density, which results in decreased mobility.

Similar to the work, where PEDOT:PSS were treated with DMSO in the closed chamber,[53] Lim et al.[80] investigated the influence of F4TCNQ doping from the vapor phase on the TE properties of P3HT matrix. Neat polymer matrix was mixed with 1:1 mixture of ortho-dichlorobenzene and chlorobenzene with further exposure of the obtained film to the F4TCNQ vapor, which is formed at 80 °C in a sealed chamber. It was estimated that polaron and bipolaron states appear and keep increasing in number with an increase of the exposure time, whereas neutral states tend to decrease. Such a shift resulted in increased mobility of the system (up to 0.6 cm² V⁻¹ s⁻¹). Since the electrical conductivity and mobility for vapor-doped films at the highest concentration of F4TCNQ were around 20 and 30 times higher than the solution doped films that had 120% of the carrier concentration, respectively, it was concluded that mobility of charge carriers dominates the contribution of the concentration leading to higher conductivity:, that is, the mobility of the charge carriers became so high that even at decreased concentration the electrical conductivity has still grown significantly. The highest Seebeck coefficient of 85 and 76 µV K⁻¹ were reached for carrier concentrations of 5 × 10²⁰ and 6 × 10²⁰, respectively. The explanation for the growth of the TE performance is, however, controversial since the decreased concentration of charge carriers, if not too high, conventionally leads to diminished electrical conductivity. The large increase of TE performance in the aforementioned work stimulated further research in that direction. Similar treatment by the F4TCNQ vapor phase is reported by Lim et al.[81] In this case, the focus of the research was the influence of order/regioregularity on TE properties (see scheme in Figure 5b). The role of the disorder is estimated through controlling the concentration of regioregular in regiorandom P3HT mixture. The increase of carrier concentration in the samples linearly correlates with the amount of RR P3HT via F4TCNQ doping from the vapor phase, and it is due to the increase of polaron energy state from the RR matrix and the anion part of F4TCNQ. In contrast to carrier concentration, electrical conductivity shows an exponential increase due to the crystallinity order from RR P3HT in the mixture and dual contribution from concentration and mobility of charge carriers. The highest Seebeck coefficient and PF are 121 µV K⁻¹ and 8 µW mK⁻², respectively. In the work done by

Zou et al.[82] the dependence of Seebeck coefficient from the energy level structure (HOMO) is studied. To dope the polymer matrix and modify the energy levels, F4TCNQ and P3HT chloroform solutions were mixed. Doping led to a decrease of HOMO energy level with respect to the Fermi level, that is, a downward shift of the Fermi level towards the HOMO edge was induced (schematically depicted in Figure 5c), thus a p-type doping is present. The slightest doping level (0.06–0.25 wt%) led to a dramatic decrease of the Seebeck coefficient from 1550 to 955 $\mu V\ K^{-1}$, while the conductivity of the polymer matrix significantly increased from 9.6×10^{-6} to 7.7×10^{-5} S cm^{-1}. Further increase of doping resulted in decreased S down to 425 $\mu V\ K^{-1}$ and improved electrical conductivity up to 8.5 mS cm^{-1}. Analysis of Seebeck coefficient versus HOMO onset binding energy showed linear dependence/correlation with the relative position of the Fermi level, which was not estimated before. It should be noted that during the fitting process the influence of numerical factor, which is related to conductivity density of states, and absolute temperature was neglected.

For P3HT polymer matrix low values of electrical conductivity always were a point of "deal breaker" when targeting the use in the TE field. Thus, its improvement is one of the main goals in the research to seek matrix application for heat conversion. Vijayakumar et al.[83] report an increase of electrical conductivity via FeCl$_3$ doping for P3HT and poly(2,5-bis(3-dodecyl-2-thienyl)thieno[3,2-b]thiophene) (C12-PBTTT) matrixes. Initially, both polymer matrixes were heat- and press-treated with a roller (see the scheme in Figure 5d) to enhance the orientation and alignment of polymer chains forming the films. The doping process took place in a FeCl$_3$/nitromethane solution, which did not affect the initial orientation of the obtained films. However, doping led to an expansion of the unit cells along the alkyl side chain direction, which demonstrates that the doping elements penetrated inside the alkyl side chain layers and, by doing so, they created two different dopant molecules: FeCl$_2$ and FeCl$_4^-$. These species affected the matrix of polymers by changing the ratio between neutral and oxidized side chains. It was estimated that the proportion of oxidized:neutral chains can be tuned up by adjusting FeCl$_3$ doping without damaging the oriented structure, which gives control over carrier density in a preferential direction. Upon doping, both polymers show a strong increase of electrical conductivity with saturation at higher concentrations, irrespective of the direction of the measurements (parallel/perpendicular to the chain direction). The C12-BPTTT exhibits a few orders of magnitude increase of electrical conductivity from 150 to ≈2.2 × 10^5 S cm^{-1}, which is due to the complete oxidation of the backbone chain. The highest achieved value of electrical conductivity for P3HT is 570 S cm^{-1} along the rolling direction. The anisotropy of properties for P3HT is lower than that of C12-BPTTT, which is explained by the orientation of domains, mixture of face-on/edge-on versus dominant face-on, respectively. The structure of the polymer is quite unique, which includes CH$_2$—O bonds with shorter bond length and smaller energy rotation compared to CH$_2$—CH$_2$ bonds. Such a structure can be used for further side-chain engineering, which can lead to higher transport properties as it is shown in the work described by Chen et al.[22] A sequential oxygen-substitution of the carbon atoms from the gamma position was reported. During the substitution process, the following polymers were formed: poly(3-(n)thiophene), where n are 2-propoxyethyl, 3-ethoxypropyl, and 4-methoxybutyl, which are named P3POET, P3EOPT, and P3MOBT, respectively (see Figure 5e). To further improve the TE performance of various polymers, the obtained films were immersed in the oxidant solution FeCl$_3$. An oxygen position within the structure of the polymers affects the overall oxidation, that is, when the O atom moves from β to ω, the side chain is more easily oxidized, which is explained by the decrease of the electron-withdrawing inductive effect, that is, the shift of a bond's electron cloud. The doping of the polymers led to the decrease of neutral states and appearance of positive bipolaron states due to the "migration" from positive polaron states. All fabricated polymers under different doping conditions were examined for TE performance and compared with pristine P3HT. For pure polymer, the highest value of conductivity was 246.1 S cm^{-1} due to the presence of both polarons and bipolarons within the system after 10 min of doping. However, P3POET and P3MOBT values are lower: 193 and 223 S cm^{-1}, respectively, due to the charge carriers in form of polarons formed during 40 s doping. The P3EOPT exhibits the highest values of electrical conductivity (250 S cm^{-1}) after immersion for 2 min, the polarons being the only charge carrier option. The behavior of the Seebeck coefficient for the pure polymer presents a decrease, whereas for all the other polymers the immersion into the FeCl$_3$ first induces the increase of S then, after the thermopower is saturated, the decrease of values for S is observed. Relatively high values of S can be achieved only at early stages of doping (shorter than 10 min), with the highest values equal to 34, 22, 26, and 61 $\mu V\ K^{-1}$, obtained for doping times of 120, 120, 120, and 20 s for P3POET, P3EOPT, P3MOBT, and P3HT, respectively. The highest PF (≈19 $\mu W\ mK^{-2}$) is reached at 40 s doping time for the polymer P3POET, in which oxygen atom is attached right next to the main ring of the polymer. Although the synthesis process is time-consuming and requires very accurate manipulation of the structure, the reported side-chain oxidation is highly perspective for tuning the TE performance of P3HT structure, that is, the creation of similar structures.

Chemical treatment is known for its huge impact on the structure and transport properties of the polymer, which is highlighted in the studies mentioned above. However, the question of the impact at various conditions such as stretching remains. This important aspect was studied: Hynynen et al.[84] reported the influence of stretching on TE properties of P3HT alongside doping with molybdenum tris(dithiolene) complex (MTDC). The stretching/orientation of the films was conducted via solid-state tensile drawing (see Figure 5f). The influence of MTDC was studied for both as-casted and stretched films for further comparison. The stretching allows increasing the electrical conductivity up to 40 times (≈12.5 S cm^{-1}) and five times (≈1.5 S cm^{-1}) in parallel and perpendicular direction, respectively. The Seebeck coefficient does not show an anisotropic behavior, though a slight decrease is observed from 138 to 112 $\mu V\ K^{-1}$. The achieved values result in a five-time increase of PF (16 $\mu W\ mK^{-2}$) along the drawing direction, in comparison to the as casted samples. The increase of anisotropy for electrical conductivity and the increasing trend dependent on stretching are explained with the formation of a 2D rectangular grid resulting in improvement of attempt frequency of hopping (including tunneling probability)

**ADVANCED
SCIENCE NEWS**

www.advancedsciencenews.com

**ADVANCED
FUNCTIONAL
MATERIALS**

www.afm-journal.de

and characteristic length scale, that is, higher carrier mobility along the drawing direction.

Apart from standard procedure of chemical treatment, which proved its effectiveness, physical treatments via impact through rolling or pulling the polymer chains were also tested. According to the results, such approach is not only more efficient for tuning TE performance, but also allows control over directional charge transfer within the samples.

4. PANI

Polyaniline (PANI) is known for its decent intrinsic values of electrical conductivity (≈ 150 S cm^{-1}) and Seebeck coefficient, which is comparable with intrinsic values of PEDOT:PSS (≈ 18 μV K^{-1}). Due to its much higher intrinsic values of electrical conductivity, compared to PEDOT:PSS and P3HT, PANI is widely investigated as a base for TE materials. The approaches mentioned above to tune the TE performance of polymer matrix are also applicable to PANI and are vastly studied.
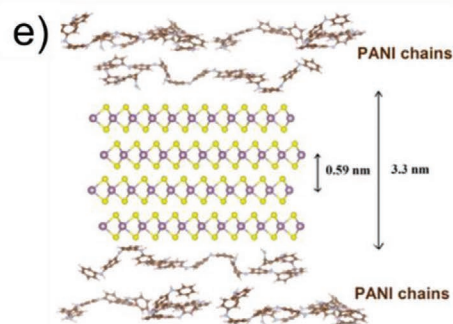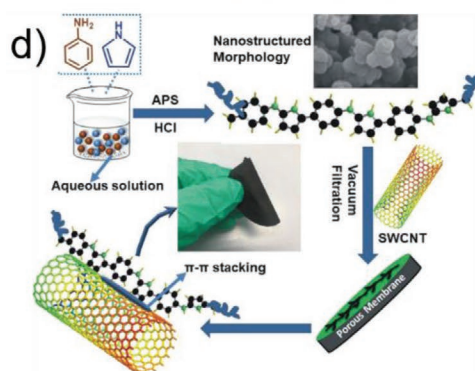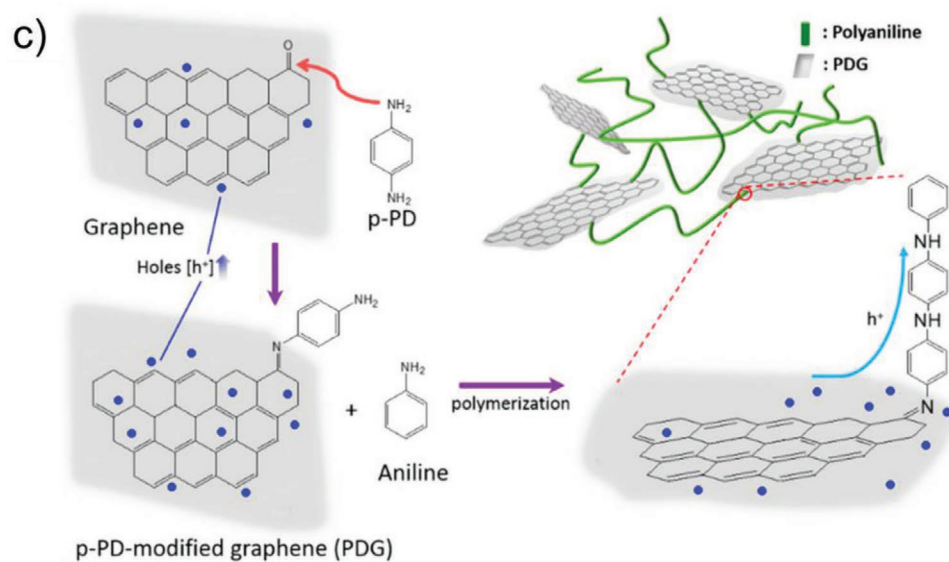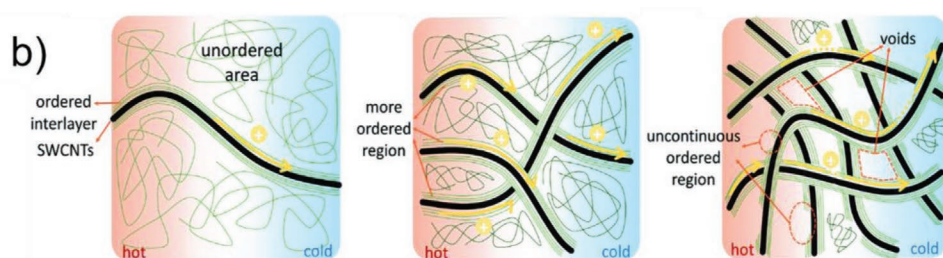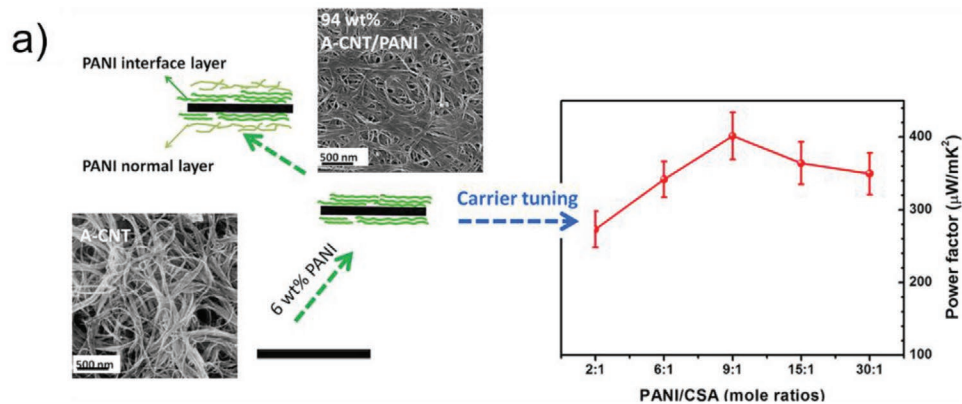
4.1. Utilization of Carbon-Based Materials

Carbon nanotubes are not easily dispersed in covalent liquids such as water and thus the functionalization (creation of −CO, −COOH and other functional groups) of their surface is required. Li et al.[85] reported the use of amine-functionalized CNT for in-situ polymerization of PANI matrix, which resulted in PF of 401 μW mK^{-2}. Initially, the strong increase of electrical conductivity up to ≈ 1870 S cm^{-1} at 57 wt % of nanotubes was observed, which is explained with formation of interlayers of PANI chains between CNTs with strong π–π interaction (see scheme in **Figure 6**a); further improvement of the functionality is inhibited due to the enlargement of interlayers up to the critical point, where interface layer of matrix is growing up to the point where PANI resembles its bulk functionality thus not contributing in transport properties the same way as the interface layer and increasing the distance between neighbor CNTs. The highest electrical conductivity and Seebeck coefficient are ≈ 2010 S cm^{-1} and ≈ 37 μV K^{-1}, respectively, with a resulting PF of ≈ 270 μW mK^{-2} at 95 wt% load. Such an abrupt increase in TE performance is due to the formation of a 3D well-connected network with CNTs as a core and PANI interface layers as a shell. The increase of the Seebeck coefficient is explained by the filtering mechanism, at which only charge carriers with high energy can surpass the formed barrier. Further adjustment of PANI doping level via treatment with camphor sulfonic acid (CSA) shows that changing the ratio between PANI/CSA from 2:1 to 30:1 leads to a decrease of electrical conductivity and a simultaneous increase of the Seebeck coefficient, resulting in the highest PF of 401 μW mK^{-2} at ratio 9:1. This behavior is due to the reduction of charge carrier concentration with a reduction of CSA presence. With a decrease of doping level, both crystallinity regions of PANI and protonated sites are decreasing, which diminishes the conductive pathway along the polymer chains. However, the crystallinity between individual chains remains and alongside the contribution from A-CNT, being an electron acceptor, can lead to a significant conductivity.

In this work, CSA was used as a post-treatment agent, but it can be also used during the process of composite preparation. Wu et al.[86] report oxidative polymerization of PANI. The composites were obtained with further mixing with CSA and various concentrations of SWCNTs. Treatment with deionized water led to an easy peeling off process of thin films from the glass substrate. Predictively, the conductivity of thin films is almost linearly increasing with the concentration of nanotubes. However, once the threshold of 70 wt % is reached, the values drop due to the uneven distribution of nanotubes and distorted surface of films. Thus, the highest value of PF, 56 μW mK^{-2}, was reached at 60 wt% load of SWCNTs. The main contribution was provided from electrical conductivity (≈ 3000 S cm^{-1}), which is far bigger than that of pure PANI or SWCNTs pure materials. A detailed analysis excluded the possibility of the formation of a percolating network within the film (see Figure 6b). The authors also excluded the possibility to claim a filtering effect of the materials as the reason for such huge increase of conductivity. As in the previous work, the results are explained with formation of an interlayer between matrix and filler, which is proven by Raman spectroscopy showing strong π–π conjugated interaction. Interlayer presence led to an increase of carrier concentration and mobility, which is due to the formation of SWCNTs network with PANI as an extra path for spreading delocalized electrons over the net.

The load factor, that is, the concentration of filler, plays a crucial role: the lower filler concentration is used to achieve the highest possible TE performance, the better it is. In the work by Lin et al.[87] the modification of graphene with p-phenediamine attachment (PDG) and further polymerization of aniline monomers is reported (see scheme in Figure 6c). The composites revealed that polymerized PANI is growing from the edges of graphene, creating a fiber-like structure between graphene sheets. Further temperature treatment at 30, 45, 60, and 80 °C showed seven times increase of electrical conductivity, compared to pristine graphene/PANI, which is due to the creation of additional holes via induction effect. The increase of graphene concentration and temperature treatment leads to higher carrier concentration and thus higher electrical conductivity up to 68 S cm^{-1} for 15 wt% 80 °C treated sample. The observed improvement of carrier mobility is due to the increased conjugated crosslinks between PDG and PANI. The highest ZT of 0.76 is reached for the sample doped with only 3 wt% of graphene and annealed at 30 °C.

It is estimated that, apart from the use of filler, the properties in PANI can be tuned via the alignment of polymer chains. Previously, such result was achieved via mechanical rolling or stretching techniques. Want et al.[88] applied SWCNTs as fillers, and introduced pyrrole into the PANI backbone to improve the alignment and, as a result, the TE performance. The introduction of pyrrole led to the strong interaction between macromolecule chains such as π–π stacking and hydrogen bonds (Figure 6d); XRD of the samples showed the improved intensity of the peaks, proving increased alignment of the obtained composites. The introduction of SWCNTs led to increased values compared to pure polymers. It is worth mentioning that the presence of pyrrole induced an increase of values by 1.6 times, compared to PANI/SWCNTs, which is reflected in the fact that the charge carrier concentration quantity rose from $\approx 30.5 \times 10^{18}$

**ADVANCED
SCIENCE NEWS**
www.advancedsciencenews.com

**ADVANCED
FUNCTIONAL
MATERIALS**
www.afm-journal.de

to 91.4×10^{18} cm^{-3}. The increase is explained by a few factors: combination of PANI and pyrrole containing π–π stacking and hydrogen bonding, which inhibits intra- and inter-chain hopping barriers of the polymer; alignment of polymer chains led to higher conductivity; nanostructure morphology of PANI and pyrrole caused strong van der Waals attraction resulting in improved carrier concentration and mobility. As a result, a high value of PF was achieved ($\approx$98 μW mK^{-2}) at 430 K, through pyrrole alignment, alongside SWCNTs incorporation.

Li et al.[90] represented a facile dedoping process through ammonium hydroxide post-treatment to tune carrier transport. Originally, the influence of SWCNTs concentration was studied: the results showed an increase of both electrical conductivity and Seebeck coefficient with increasing content of filler. The growth of electrical conductivity is observed up to $\approx$3020 S cm^{-1} at 73 wt% of filler, after which the values decreased. The Seebeck coefficient keeps increasing constantly with the increase in concentration. The highest PF is 234 μW mK^{-2} at 73 wt%, followed by an abrupt decrease of conductivity. The authors give no explanation about the mechanism leading to the improved properties. The following de-doping with ammonium hydroxide leads to the change of benzenoid rings into quinoid units alongside the change from expanded to the coil-like structure. This reflected in restrictions in charge flow through ordered PANI regions and in increased interface barrier between polymer and nanotubes, resulting in increased Seebeck coefficient and decreased electrical conductivity. The optimal PF of 345 μW mK^{-2} was achieved for the sample treated for 1 min with 0.5 м ammonium hydroxide. Generators based on the obtained materials exhibit output power of 1.11 μW, which was generated at the load resistance of 20 Ω.

Utilization of carbon-based fillers can be more efficient if the interlayer concept is implemented to contribute to the transport properties. However, for that an appropriate change of the carbon material surface is required. Such approach should be considered alongside application of redox process or doping/dedoping of the system as shown in the work by Li.[91]

4.2. Organic/Inorganic Composites

In the frame of the research for the development of advanced TE materials with improved performance, MoS$_2$ represents a viable candidate, already exploited in the field of photovoltaics.[91] In fact, 2D MoS$_2$ can be also utilized as a part of TE composites. In the work by Mombru et al.[89] MoS$_2$ nanosheets were introduced into the PANI matrix in the 5, 10 and 15 wt % concentrations via suspensions mixing. The structure of the composites is represented in Figure 6e. Electrical conductivity increases with the concentration of nanosheets from 1.89 S cm^{-1} (pure PANI) to 2 S cm^{-1} and up to 54 S cm^{-1} at 10 wt % load of filler; the values are much higher than that reported for pure MoS$_2$ ($\approx$10^{-4} S cm^{-1}). Such change of transport

properties is related to the increased density of charge carriers, which is reflected in improved polaron energy states estimated by Raman spectroscopy. The Seebeck coefficient is negligibly increasing up to $\approx$5.3 μV K^{-1} at a 15 wt% load. No explanation for the trend of the Seebeck coefficient is provided. The PF value of 0.007 μW mK^{-2} at 15 wt% doping is 3.5 times higher compared to non-doped PANI.

Other nanomaterials were also used to boost the TE performance of polymer matrixes. Silver-based nanosystems were investigated due to their intrinsic high transport properties. Du et al.[92] used PSS as a suspension stabilizer with Ag nanowires as filler. The presence of PSS makes the solutions of PANI in deionized water stable for at least one month without additional steering. Once the PSS is added to the system, the degree of disorder increased, due to the strong interaction between PANI and PSS. Since PSS is an insulator, the overall conductivity of PANI:PSS is lower than that of pure PANI. However, further incorporation of Ag NWs leads to the slow increase of conductivity ($\approx$16 S m^{-1}) up to the 12.5 wt% of nanowires, which is an estimated threshold for Ag NWs concentration. Above the threshold, the conductivity increases sharply, reaching values in the 10^3 S m^{-1} range, which indicates the formation of an Ag NWs percolating network. The PEDOT:PSS ratio plays a significant role in tuning the transport properties. The 1:5 PEDOT:PSS ratio even at higher load exhibits conductivity lower than that of 1:10; this behavior can be explained with the decrease of carrier scattering at the interface Ag NWs/PANI:PSS at higher concentration of filler. Seebeck coefficient values are 220 and $\approx$290 μV K^{-1} for 1:10 and 1:5 ratio, respectively, indicating that the incorporation of PSS enables the energy filtering effect. Further addition of Ag NWs increases the values of S up to $\approx$670, and $\approx$400 μV K^{-1} at a 9 wt% for 1:10 and 1:5 ratios, respectively. The highest PF is 0.85 μW mK^{-2} for PANI: PSS/Ag NWs with 9 wt% of load and 1:5 PANI:PSS ratio.

As discussed, up to now, the most conventional approach to tune the TE performance of polymers is the introduction of a single filler, either organic or inorganic. More advanced strategies include the use of double doping, that is, the creation of ternary systems, where two fillers can be added into a single polymer matrix. In the work by Erden and co-workers,[93] the combined effect of amine-functionalized CNTs (a-CNT) and TiO$_2$ nanoparticle doping is studied on the TE performance of PANI. Incorporation of a-CNT at 70 wt% into the matrix led to a significant increase of electrical conductivity up to 2733 S cm^{-1} and Seebeck coefficient up to $\approx$18 μV K^{-1}. The increase of both these parameters is due to a variety of features: the growth of PANI from amine groups on the surface of CNTs; the high intrinsic electrical conductivity of a-CNTs; the longer electron delocalization along with C–N bonds. The described changes reflect in improved carrier mobility and concentration up to 6 and $\approx$2.6 times, respectively. To further boost the TE performance, the introduction of TiO$_2$ nanoparticles was studied to achieve filtering effect at the interfaces TiO$_2$/a-CNT and

Figure 6. a) Formation of interlayers and influence on TE performance, Reproduced with permission.[85] Copyright 2018, Elsevier Ltd. b) Scheme of percolation threshold on the structure (formation of voids within the material), Reproduced with permission.[86] Copyright 2018, Royal Society of Chemistry. c) Scheme of PANI growth from the graphene edges, Reproduced with permission.[87] Copyright 2018, American Chemical Society. d) Incorporation of new chains within the system with formation of π–π stacking, Reproduced with permission.[88] Copyright 2019, Elsevier Ltd. e) Incorporation of MoS$_2$ between PANI chains. Reproduced with permission.[89] Copyright 2018, Springer US.

TiO$_2$/PANI, due to the work function barrier around ≈0.3 eV. The study of the ternary systems showed that an increase of TiO$_2$ leads to an inverse trend for electrical conductivity (decreasing) and Seebeck coefficient (increasing), reflecting in lower values of both mobility and concentration of charge carriers, resulting in the highest PF of ≈114 µW mK^{-2} at 30 wt% load TiO$_2$ for composite with 70 wt% concentration of a-CNTs.

As shown for other polymer matrixes, the use of conventional TE materials or their derivatives is a promising strategy to improve TE performance, especially if combined with chemical treatment. In the work by Ju et al.[94] the fabrication of dodecylbenzene sulfonic acid-doped (DBSA) PANI-coated SnSe$_{0.8}$S$_{0.2}$ nanosheets is reported. The thermoelectric properties were studied with respect to the number of PANI coating on nanosheets. The outstanding charge transport properties of PANI are originated from DBSA doping: the higher the number of coating cycles, the higher the electrical conductivity and the lower the Seebeck coefficient are. The highest and optimum PF (≈250 µW mK^{-2}) is reached for the sample with two coating cycles of PANI. Flexible TEG was fabricated via the addition of PVDF into the dimethylformamide solution. With a ratio 2:1 of PANI-SnSeS:PVDF a PF of ≈110 µW mK^{-2} for TEG was reached. The flexible material showed no decrease of the PF after up to 1000 bending cycles, demonstrating high durability and PF of ≈134 µW mK^{-2} at 400 K. By applying similar strategy, Mitra et al.[95] studied the polymerization/growth of aniline monomers on the surface of Bi$_2$Se$_3$ nanoplates resulting

in 2D composite materials. The presence of nanoplates led to ≈4 times enhancement of carrier mobility and a slight decrease (19%) in carrier concentration. These features resulted in an increase of Seebeck coefficient and electrical conductivity; which led to the improvement of PF up to ≈29 µW mK^{-2} at 30 wt% of nanoplates, 30 times more than that of pure PANI. The improvement is attributed to the change in the charge carrier's behavior and energy filtering effect. The slight increase of thermal conductivity is negligible and the overall values of the figure of merit are 0.046 and 0.18 at 300 and 410 K, respectively.

The conventional use of Te nanorods (NR) is known to boost TE performance via adjustment of charge carrier's concentration. Wang et al.[96] studied the change of TE properties as a function of the annealing temperatures for pure and Te NR doped films with 60 wt% nanorod concentration. Annealing of the samples at 160, 180, and 200 °C (see **Figure 7**a) showed partial loss of secondary dopants from the surface. Seebeck coefficient increased from ≈71.5 to 264 µV K^{-1} during annealing process at 200 °C. The electrical conductivity decreased from 4040 to 0.32 S cm^{-1} for as prepared and annealed samples, respectively, due to the decrease and partial disappearance of well-defined crystalline structure at higher annealing temperature, which is explained by the melting of the crystallites. The above-mentioned changes affected both mobility and concentration of charge carriers. Annealing of the Te NR–treated sample exhibits an improved crystallinity of NR, that is, recrystallization of Te along (110) plane. Despite the decrease of electrical
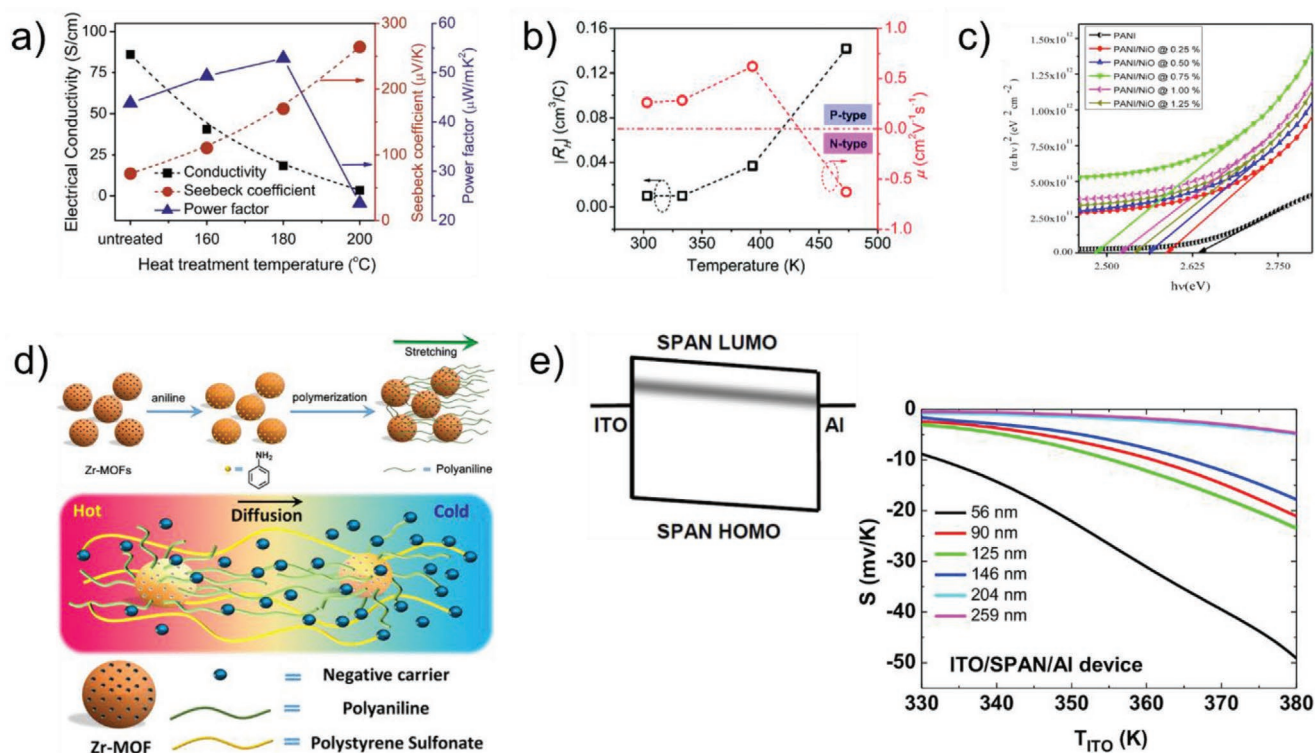
Figure 7. a) Influence of annealing temperature on TE performance. Reproduced with permission.[96] Copyright 2018, Elsevier Ltd. b) Competition between holes and electrons with increasing temperature. Reproduced with permission.[97] Copyright 2019, Royal Society of Chemistry. c) Influence of NiO concentration on the bandgap of composite. Reproduced with permission.[98] Copyright 2019, Elsevier Ltd. d) Creation of hybrid fillers Zr-MOF/PANI/PSS, Reproduced with permission.[99] Copyright 2019, American Chemical Society. e) SPAN effect on the electronic structure. Reproduced with permission.[100] Copyright 2019, Elsevier Ltd.

**ADVANCED
SCIENCE NEWS**
www.advancedsciencenews.com

**ADVANCED
FUNCTIONAL
MATERIALS**
www.afm-journal.de

conductivity, optimal values of PF (≈ 53 μW mK^{-2}) are achieved for 180 °C treated sample exhibiting an enhancement of 20% compared to the values of the as-prepared film. Another element, which is known to highly contribute to TE performance is Bismuth (Bi) and Bi-based materials. In the work by Wang et al.[97] the use of Bi_2S_3 nanorods to fabricate n-type composites with elevated TE performance was reported. PANI, doped with CSA, was used as matrix with addition of various concentration of Bi_2S_3 nanorods. The Raman analysis showed some cross-linked structures of polymer with slight blue shift after thermal treatment, which leads to partial dedoping of CSA from the system. It appeared that the core–shell structure formed during the synthesis with the arrangement of hydrogen bonds or Van der Waals forces between nanorods and polymer matrix, creating additional polaron energy states. Electrical conductivity of the samples decreases from 81 to ≈ 5 S cm^{-1} with the growth of filler concentration up to 90 wt % load, due to the low intrinsic conductivity of the compounds. The decrease of conductivity at elevated temperatures is due to the decrease in crystallinity and to the loss of emeraldine sequence. The studied sample exhibited change of doping nature from p- to n-type at the temperature of 483 K. The change of nature can be explained with increased contribution of electrons to the Seebeck coefficient and eventual dominance of electrons over holes as major carrier charges (Figure 7b). Moreover, the higher the concentration of NR, the lower the transition temperature of carrier charges is. The highest Seebeck coefficient of -163 μV K^{-1} is achieved at 70% concentration of Bi_2S_3. Once the transition takes place, the hybrid composites preserve their n-type nature, that is, electrons acts as majority conduction carriers. The highest PF is ≈ 7 μW mK^{-2} at 80 wt% of Bi_2S_3 in the system. TEG of the obtained samples were formed with p-type PANI/Te hybrid films. The highest output voltage of ≈ 141 mV was achieved at $\Delta T = 90$ K.

Wide bandgap materials in small quantities can significantly improve the TE performance of the polymer matrixes. Sarkar and co-workers[98] studied the effect of addition of NiO as a wide bandgap semiconductor to the aniline monomers solution during polymerization, resulting in a composite with concentrations of filler from 0.25% to 1.25%. In-situ polymerized composites showed that NiO can serve as the bridge to interconnect polymer chains, preventing the crystal growth, which disturbs the transport of charge carriers. The growing redshift of the bandgap (Figure 7c) was observed for samples with increasing concentrations of filler up to 0.75%, followed by blue shift once the threshold was exceeded. An increase of electrical conductivity was observed for samples doped with NiO up to 0.75% with the highest achieved values equal to ≈ 0.14 S cm^{-1}, 17 times larger than that of pure PANI. The initial increase of conductivity is due to the effective extension of the chain length through NiO, which serves as bridge. However, excess in NiO concentration forms insulating barriers, which prevent hopping of charge carriers between favorable sites. The Seebeck coefficient exhibits the same trend as a function of the concentration of NiO, which is evident at elevated temperature. The highest PF of 1.25 μW mK^{-2} is obtained for the sample with 0.75% NiO content at 110 °C.

Hybrid composites demonstrated higher TE performance compared to pure materials. The use of hybrid (organic/inorganic) fillers has the potential to lead to even higher improvement thanks to various factors such as additional interface,

tuning of electronic band structure, and modulation of charge carrier concentration. Lin and co-workers[99] created a hybrid filler (Figure 7d) via in-situ oxidative polymerization of aniline with polystyrene sulfonic acid as a dopant, and in presence of zirconium-based metal-organic framework (Zr-MOFs). Incorporation of PANI led to the formation of a threadlike structure of PANI attached to Zr-MOFs, that is, zirconium crystals, which are interconnected with the polymer chains. The attached polymer exhibits higher crystallinity, compared to the reference, due to the high stirring speed during polymerization. The Seebeck coefficient highly increases up to $-17\,780$ μV K^{-1} and changed its nature from p- to n-type. That is due to the decreased bandgap of the system through the overlap of electron clouds from Zr-MOFs and nitrogen atoms of PANI, alongside the increased concentration and mobility of charge carriers. The increase of the Seebeck coefficient is also supported by the contribution of the Soret effect from the polyelectrolyte of PAn/PSS, playing the role of electron storage at the cold end of the sample. The improved crystallinity of PANI and the concentration of Zr-MOFs led to enhanced electrical conductivity. The highest PF of 664 μW mK^{-2} was achieved for the sample with 20 wt% of Zr-MOFs.

Organic/inorganic systems proved themselves as a promising approach in TE field. However, the utilization of the standard system "matrix/filler/chemical treatment" is not enough to boost TE performance even higher. In turn, the use of multiple filling materials (ternary systems) can be considered as a next step in future research, since they exhibited higher transport properties and applicability in TE field by reaching PF values above 600 μW mK^{-2}, which is a threshold for systems based on a single filler.

4.3. Chemically Modified Composites

The polymer matrix per se exhibits TE performance way below the required ones for actual application due to the variety of reasons: low number of polaron, bipolaron energy levels, low concentration and mobility of charge carriers, inhomogeneous surface, and so forth. The mentioned reasons usually driven by the redox potential of the system, can be ideally alleviated and regulated via base/acid/ILs treatments or doping/dedoping/redoping of the system. The direct growth of the polymer matrix on top of the surface gives certain advantages. The growth of sulfonated polyaniline (SPAN), which is PANI with sulfonated phenyl rings, thin film on glass/ITO substrate was studied.[100] It was estimated that the thicker the layer of the SPAN, the more inhomogeneous the surface tends to be, affecting the transport properties of the system. For the thinnest SPAN (56 nm), the highest Seebeck coefficient was achieved (≈ 50 mV K^{-1} at 380 K). Authors were not able to give a univocal explanation of the results, but, according to the literature, high mobility of charge carriers in the direction of electric current is a major requirement for giant Seebeck coefficient. Since the transport properties were measured in vertical direction it was suggested that once the device is heated up from the ITO side, the temperature-dependent electron energy occupation fraction allows a higher number of electrons reaching the SPAN LUMO (the mechanism and effect are sketched in Figure 7e).

**ADVANCED
SCIENCE NEWS**

www.advancedsciencenews.com

**ADVANCED
FUNCTIONAL
MATERIALS**

www.afm-journal.de

There are certain papers where the TE performance is record-breaking, but the mechanisms are not explained thoroughly, as shown in the previous one; in contrast to them. The work by Hotra-Romaris et al.[101] focuses on the detailed explanation of the mechanisms behind the changes of the TE performance under sulfonic acids. The PANI samples were synthesized by an indirect route, that is, "dedoping-redoping." First, the dedoping process was done on PANI-HCl via 1 M NH$_3$, then the obtained PANI-base was redoped by either 5-sulfoisophatalic acid sodium salt (NaSIPA) or dodecylbenzene sulfonic acid-doped (DBSA). DBSA treated films exhibit electrical conductivity from 4 to 70 times higher than that of NaSIPA one. Further increase of dopant concentration makes this difference even more abrupt, reaching 30 and 0.5 S cm^{-1} at 1.25 and 0.75 M for DBSA and NaSIPA, respectively. Such changes are due to the increase of doping level: improvement from ≈0.25 to ≈0.8 M for DBSA and up to 0.24 protonation degree for NaSIPA. The original form of the polymer is a benzoid-type ring, which can be changed to a quinoid one; the difference between the two is the changed position of the double bonds; the quinoid one exhibits higher transport properties. The observed changes of transport properties reflect in the results from FTIR analysis, where the change of relative intensity between quinoid and benzoid bands (I$_{Q/B}$) is clearly detected, moving from 0.93 to 0.75 for DBSA treatment and being stable (0.91) after NaSIPA treatment. The more quinoid systems are present, the easier the protonation is. During the treatment, the concentration of bipolaron, polaron, and electron delocalization states is increasing. The relative variation is higher for DBSA, compared to NaSIPA. Additional contribution to the increase of conductivity is due to the formation of a layered structure within the composite; more planar chain conformation with reduced torsion angles between the phenyl rings and the plane of backbones is caused by the rigidity of the PANI chains due to the electronic repulsion of DBSA and the polar nature of PANI. The values of the Seebeck coefficient are constant (≈1 µV K^{-1}) for DBSA treated films, irrespective of dopant concentration and temperature growth, whereas the values decrease with increased acidity and increase with growing temperature for NaSIPA films. The low values of DBSA films are due to the polaronic hopping, in contrast to NaSIPA treated films that exhibit diffusive (metallic-like) conduction and variable range hopping, that is, the hopping of charge carriers in an extended temperature range. The thermal conductivity shows opposite behavior, with respect to the Seebeck coefficient: DBSA-PANI samples exhibit no correlation with temperature change, while, once the doping level starts increasing, the thermal conductivity shows an abrupt jump from ≈0.15 to ≈0.6 W mK^{-1}. The samples treated with NaSIPA show a thermal conductivity, which is independent from the doping level. With the increase of temperature, a small fluctuation of values was observed within the experimental error (0.22 ± 0.02) W mK^{-1}, which is interpreted as an absence of changes or a negligible variation, which can ignored. The absence of correlation between thermal and electrical conductivity is explained with Van der Waals or H-bonding contact between molecules, which cause strong phonon scattering and negligible contribution from charge carriers, thus resulting in a thermal conductivity mainly dictated by the lattice vibrations. The highest values of ZT for PANI-DBSA and PANI-NaSIPA

are 3.2×10^{-6} and 1.0×10^{-5} at 1 and 0.1 M doping levels, respectively, showing that the de-doped PANI-base should be re-doped with NaSIPA for higher TE performance. These results are not among the highest reported by any means; however, the comprehensiveness of the study is an excellent example of a solid proof for the acquired results.

5. Nonconventional Approaches

In this section, we are focusing on the description of nonconventional approaches to boost TE performance of the polymer matrixes for creating usable devices, mainly generators. Conventional approaches typically include the following treatments: the polymer matrix is either treated/incorporated with chemicals/fillers or, after modification, is used in the stacked composites to improve efficiency of heat to electrical energy conversion. In the studies described in this section, instead, the authors focused on incorporation of modified polymer matrixes within textiles toward creation of portable and wearable power generators. Such approach, if successful, that is, with high TE performance, can be used for direct fabrication of wearable clothes/TE generators. In the work by Jia et al.,[102] the authors report covering commercial textile with PEDOT:PSS via vapor phase polymerization (VPP). The process of incorporation of TE material into the textile directly affects the final performance of the composite system. Various parameters should be adjusted for the successful and efficient utilization of the obtained textiles. The transport properties of the manufactured materials were studied as a function of the number of deposition cycles and utilized textiles. The lowest resistivity (≈150 Ω cm^{-1}) is reached for the cotton thread covered with PEDOT at three cycles, after which it remains stable. The behavior is explained by the fact that three cycles are necessary to fully cover the textile via VPP. Stability tests versus temperature and water showed that the resistance of the system does not change heating up to 100 °C for 30 min, with further increase of the resistance, when the temperature exceeds that threshold. The behavior can be explained with the chemical reduction process of the polymer matrix and the formation of microcracks on the surface of the textiles. The stability under water testing is superior, compared to other studies, due to the limited increase of the resistance (maximum increase by factor two for 12 h washing), whereas other works show up to 8-fold increase of the resistance. Such stability is achieved due to the strong adhesion of PEDOT to textiles through multiple in situ VPP processes. The TE generators showed maximum output power of 62 nW at $\Delta T = 100$ K and a corresponding output density of 42 nW cm^{-2} with effective area 1.5 cm^2. Achieved output power is not the highest reported in the literature and the ΔT at which it was acquired is too high. Typical range is in the range from 10 to 20 K, which should result in lower values. However, the area of the final wearable TE generator is enough to power small electronic devices. Basically, the current and other similar types of works are focused on a direct implementation in the daily life; however, the majority of similar published results are not yet efficient enough.

The comparison of the revised research works is represented in **Table 1**, where there are TE properties, used polymers,

**ADVANCED
SCIENCE NEWS**

www.advancedsciencenews.com

**ADVANCED
FUNCTIONAL
MATERIALS**

www.afm-journal.de

Table 1. Comparison of the functional properties of different systems from the recent literature.

Main polymer	Filler	Chemical doping	Mechanism	Seebeck coefficient [$\mu V\ K^{-1}$]	Electrical conductivity [$S\ cm^{-1}$]	Thermal conductivity [$W\ K^{-1}\ m^{-1}$]	Power factor [$\mu W\ K^{-1}\ m^{-2}$]	ZT	Output voltage [mV]	Output power [nW]	Ref.
PANI			Incorporation of oxygen in backbone	35	140		19				Chen et al.[22]
PEDOT:tos	CNT	TDAE	Ionic transport	14 000	250	0.6	1200	0.7			Choi et al.[29]
PEDOT:PSS	CNT	Hydrazine, PEI	Change of the major charge carriers	30	1000	–	p-type 83 n-type 113	–			Kim et al.[31]
PEDOT:PSS	FCNT	EG, DMSO		46	250	–	56	–			Yusupov et al.[32]
PEDOT:PSS	FCNT	EG, DMSO	Number of layers	46	250	–	56	–			Yusupov et al.[33]
PEDOT:PSS	SWCNT	DMSO, NaOH	Dedoping	55	1700	0.4–0.6	526	0.39			Liu et al.[34]
PEDOT:PSS	SWCNT		Vacuum filtration	45	550	0.26	105	0.12			Jiang et al.[36]
PEDOT:PSS	SWCNT, PEDOT:PSS nanowire		Energy filtering	36	2500		352		5	414	Liu et al.[37]
PEDOT:PSS	SWCNT	SDS	Core–shell, 3D network	50	680		160		1.8		Wang et al.[42]
PEDOT:PSS, PDDA	DWCNT, graphene		sandwich-like structure	70	340		168				Stevens et al.[43]
PEDOT:PSS	Graphene			17	1000		30		4	30.9	Liu et al.[45]
PEDOT:PSS	Te, Cu_7Te_4		3D network	163	42	0.198	112	0.1	31.2	95	Lu et al.[46]
PEDOT:PSS	Te-s-Se		Charge hopping	120	150		222				Ju et al.[48]
PEDOT:PSS	Te	H_2SO_4, NaOH		65	561		240		0.8		Ni et al.[49]
PEDOT:PSS	Ge thin film		Kraut's method	398			154				Lee et al.[50]
PEDOT	$Cu_{12}Sb_4S_{13}$	OLA	Hole-phonon scattering	18	278.36	0.29	9.6	0.0098			Lim et al.[51]
PEDOT:PSS	Bi_2Te_3	PSVA	Barrier offset on the interfaces	45	1000	0.29	205	0.2			Kim et al.[52]
PEDOT:PSS	Black phosphorus	DMSO	Energy filtering	15.5	1446		36.2				Novak et al.[53]
PEDOT:DBSA	Te			30	1380		104				Shi et al.[55]
PEDOT:PSS	Bi_2Te_3 NW	SDS, EG	3D network	24.5	124	0.047	7.45	0.048		130	Thongkham et al.[57]
PEDOT:PSS	Cu_2Se NW		Heat scattering/ energy filtering	51	1047	0.25–0.3	270	0.3	15	320	Lu et al.[58]
PEDOT:PSS			Surface polarization	120	5		96				Peng et al.[59]
PEDOT:PSS	IL	H_2SO_4, NaOH	Hetero-structure, Soret effect	65	1500	0.2–0.5	754	0.75			Fan et al.[60]
PEDOT:PSS	PSSH/ PSSNa	H_2SO_4, NaOH	Hetero-structure, Soret and filtering effects	≈44/48	2120/1732		401				Guan et al.[66]
PEDOT:PSS	IL		Soret effect	42	420		82				Saxena et al.[67]

Table 1. Continued.

Main polymer	Filler	Chemical doping	Mechanism	Seebeck coefficient [μV K^{-1}]	Electrical conductivity [S cm^{-1}]	Thermal conductivity [W K^{-1} m^{-1}]	Power factor [μW K^{-1} m^{-2}]	ZT	Output voltage [mV]	Output power [nW]	Ref.
PEDOT:PSS	MOF, hydrogel	PSSH	Soret effect, increased amount of PSS	16 200			7600		81		Kim et al.[68]
PEDOT:PSS	BSA	DMSO, HZ	Phase separation		1996		203		4.6		Wang et al.[69]
PEDOT:OTf		NaOH	RedOx, doping/dedoping	49	2342		570				Yao et al.[70]
PEDOT:PSS	IL	Mixture of IL	Soret effect	17	520		15				Mazaheripour.[71]
PEDOT:PSS		N$_2$ gas		30	1200		94				Zar Myint et al.[72]
PEDOT:PSS	PEIE	H$_2$SO$_4$	Doping/dedoping	24	2800		133				Li et al.[73]
PEDOT:PSS		H$_2$SO$_4$, NaOH	Doping/dedoping	25	715		46		7.1	157	Ni et al.[74]
P3HT	CNT	Iodine	Redoping	29	1722		148				Tonga et al.[75]
P3HT	SSWCNT		Energy filtering, tunneling	39	130		21		6.2	68.3	Kang et al.[76]
P3HT	Sb$_2$Te$_3$	F4TCNQ		102	1.78		1.6				Jang et al.[77]
P3HT	MoO$_3$, PbS quantum dots		Polarization effect	105	0.014		0.2				Sun et al.[78]
P3HT		F4TCNQ vapor	Improved crystallinity	60	10		32.7				Hynynen et al.[79]
P3HT		F4TCNQ vapor		85	180		27				Lim et al.[80]
P3HT		F4TCNQ	Structural ordering	110	13		10				Lim et al.[81]
P3HT		F4TCNQ	HOMO edge adjustment	424	0.0085						Zou et al.[82]
P3HT		FeCl$_3$, I$_2$ doping	Orientation via rubbing	9.4	220 000		2000				Vijayakumar et al.[83]
P3HT			Stretching of polymer chains	112	13		16				Hynynen et al.[84]
PANI	A-CNT	Sulfonic acid	Interlayer		2012		401				Li et al.[85]
PANI	SWCNT		Percolation threshold	12	4000		100				Wu et al.[86]
PANI	Graphene	PDG	Growth from graphene	604	14.5	0.22		0.74			Lin et al.[87]
PANI	SWCNT		$\pi-\pi$ stacking	50	375		98.5				Wang et al.[88]
PANI	MoS$_2$		MoS$_2$ between PANI layers	5.3	2.5		0.007				Mombrú et al.[89]
PANI	SWCNT	Ammonia	Dedoping	35	2400		345		9 mV	1.1 μW	Li et al.[90]
PANI:PSS	Ag NW			380	0.16		0.85				Du et al.[92]
PANI	CNT, TiO$_2$		Energy filtering effect	18	2733		114				Erden et al.[93]
PANI	SnSeS, PVDF		PANI-SnSeS network	370	10		134				Ju et al.[94]
PANI	Bi$_2$Se$_3$		2D VRH	188	30	0.25	107	0.18			Mitra et al.[95]
PANI	Te NR		Annealing	170	20		54				Wang et al.[96]

**ADVANCED
SCIENCE NEWS**
www.advancedsciencenews.com

**ADVANCED
FUNCTIONAL
MATERIALS**
www.afm-journal.de

Table 1. Continued.

Main polymer	Filler	Chemical doping	Mechanism	Seebeck coefficient [μV K⁻¹]	Electrical conductivity [S cm⁻¹]	Thermal conductivity [W K⁻¹ m⁻¹]	Power factor [μW K⁻¹ m⁻²]	ZT	Output voltage [mV]	Output power [nW]	Ref.
PANI	Bi₂S₃, Te NR		Competition between nature of charge carriers	42	40		0.05		140 mV		Wang et al.[97]
PANI	NiO		Wide band gap	331			1.2		34		Sarkar et al.[98]
PANI	Zr-MOF		Soret effect, stretching, hybrid filler	−17 780	2.1	0.46	664				Lin et al.[99]
SPAN				−50 000	1 × 10⁻⁶						Penteado et al.[100]
PANI		DBSA, NaSIPA		40	1	0.25		0.0001			Horta- Romarís et al.[101]
PEDOT			Stretching	16						5	Jia et al.[102]

utilized fillers and chemicals, main mechanisms behind the achievements, and output voltage/power.

6. Conclusions and Perspectives

The present progress report is focused on recent research works in the field of TE nanomaterials based on polymer matrixes. The new frontier in the research for efficient TE materials is represented by polymers due to their valuable properties.[23] Among the variety of matrixes, the three most promising and mainly used are: poly(3,4-ethylenedioxythiophene) polystyrene sulfonate (PEDOT:PSS), poly(3-hexylthiophene-2,5-diyl) (P3HT), and polyaniline (PANI).

Among all the possible mechanisms boosting the TE performance, the Soret effect and the energy filtering effect seem the most effective strategies in reaching PF of the order of mW instead of μW, which is usually a case in polymer-based materials. Application of Soret effect requires additional efforts due to the necessity to form a system with an easy access and mobility[103] of ions. Utilization of both Soret and energy filtering effects in the same system can be even more efficient.

Application of composite organic/inorganic systems proved themselves as a promising approach in TE field. However, the utilization of the standard system "matrix/filler/chemical treatment" is not enough to boost TE performance even higher. In turn, the use of multiple filling materials (ternary systems) and hybrid fillers can be considered as a next step in future research, and they have proven to be exceptionally effective for n-type materials. It seems that the more materials are used with appropriate energy offsets in the interfaces of compounds the more efficient the system can be.

Utilization of chemical agents to affect the electronic structure is one of the most efficient, if used alongside the implementation of fillers within the studied polymers. Recently, carbon nanotubes have been often used due to possibility of forming 3D network within the matrix. This technique is mainly focused on improvement of electrical conductivity. Usage of carbon-based fillers can be more efficient if the interlayer concept, which is implemented to contribute to the transport properties.

Apart from standard procedure of chemical treatment, which proved its effectiveness, physical treatments via impact through rolling or pulling the polymer chains were also tested. According to the results, such approach is not only more efficient for tuning TE performance, but also allows control over directional charge transfer within the samples.

The use of conventional semiconductor, despite the relatively high TE efficiency, have not exceeded the functionality exhibited by systems, where organic fillers were used, in the same temperature range. It seems that utilization of only the inorganic systems is not as promising as other approaches at least in the state-of-the-art TE composites in the low temperature range.

The results prove that polymer based TE are of great interest and of high importance in the field of electricity production from waste heat. They have proven to be promising materials due to the reached high values of TE performance and the possibility to switch electronic conductivity between p- and n-type, through simple chemical treatment. High PF were reached through exploitation of new mechanisms and combination of different routes, resulting in unprecedented values of thermopower and output parameters (voltage, power). Problems still exist, to be solved for a transit from laboratory to manufacturing, such as the creation of efficient n-type materials, the scale up of the preparation methodologies, the punctual investigation of the TE properties in the cross-plane direction, which seems the natural one for a real life application, where the temperature gradient is set through the cross section of the operating device.

Based on the achieved results and the literature of conventional thermoelectric materials, it can be concluded that the main mechanism and very promising one is energy filtering. This mechanism allows achieving the highest TE performance even at a very low concentration of a filler agents. However, unlike the conventional materials, the polymer-based ones due to their structure, can benefit from application of the Soret effect. To our opinion, this effect is currently underrated and

can play a great role in the future studies. The most advanced and high performance TE material can be achieved by managing to create conditions where both effects could take place, that is, presence of fillers with band energy offset from the polymer matrix and moving though the materials ions. Based on the aforementioned description, we suggest a route that may help overcoming the described issues.

The route is based on the use of the Soret effect since it showed remarkable enhancement of transport properties. Manufacturing of highly porous structure (scaffold) of polymer matrix with controlled directionality of chains and further incorporation of small ions like H^+ can lead to an outstanding improvement of transport properties once utilized at high humidity, due to the contribution to the mobility of charge carriers in form of ions. Additional utilization of various nanostructures of organic (graphene and/or nanotubes) and inorganic (NWs, quantum dots, nanosheets) nature can contribute to the increase of the concentration of charge carriers. In this approach, one can trace the usage of filler concept: the presence of PSS and water molecules results in an advantage, whereas it is usually a drawback, thanks to the ion contribution to electron conduction, and the possibility of achieving a directional charge flow, obtained either by synthesis process or mechanical effect. The formation of scaffold-like system can be an advantageous strategy for solving the issue of scaling up composite systems for TE application.

Thermal conductivity behavior in this scenario is difficult to predict, that is, thermal conductivity involves electronic and lattice parts. Formation of scaffold-like systems can increase the order of the formed structures, that is, the creation of preferable direction of chains, implying an improved lattice thermal contribution. However, since such system probably will not be used per se, but alongside the filler incorporation and chemical treatment, the negative contribution of the lattice thermal conductivity could be diminished. One should note that the phonon part in the doped disordered conjugated polymers does not exhibit the same significant influence on the transport properties as it occurs in the inorganic systems, meaning that the electron-phonon coupling is less influential compare to electron coupling.[104] Suggested route should give high TE yield because of the Soret effect and scaffold structure.

Overall, composite TE based on polymers represent a viable route to contribute exploiting waste heat in the low temperature range for energy production, with unique technical features, which are not offered by inorganic counterparts, and which make them appealing for a series of end user applications.

Conflict of Interest

The authors declare no conflict of interest.

Keywords

[1] V. Gaigalis, V. Katinas, *Renewable Energy* **2020**, *151*, 1016.
[2] K. Dong, G. Hochman, Y. Zhang, R. Sun, H. Li, H. Liao, *Energy Econ.* **2018**, *75*, 180.
[3] M. S. Nazir, A. J. Mahdi, M. Bilal, H. M. Sohail, N. Ali, H. M. N. Iqbal, *Sci. Total Environ.* **2019**, *683*, 436.
[4] Z. Zoundi, *Renewable Sustainable Energy Rev.* **2017**, *72*, 1067.
[5] M. deCastro, S. Salvador, M. Gómez-Gesteira, X. Costoya, D. Carvalho, F. J. Sanz-Larruga, L. Gimeno, *Renewable Sustainable Energy Rev.* **2019**, *109*, 55.
[6] I. Malico, R. Nepomuceno Pereira, A. C. Gonçalves, A. M. O. Sousa, *Renewable Sustainable Energy Rev.* **2019**, *112*, 960.
[7] N. Sánchez-Pantoja, R. Vidal, M. C. Pastor, *Renewable Sustainable Energy Rev.* **2018**, *98*, 227.
[8] D. Benetti, E. Jokar, C. H. Yu, A. Fathi, H. Zhao, A. Vomiero, E. Wei-Guang Diau, F. Rosei, *Nano Energy* **2019**, *62*, 781.
[9] D. A. Vallero, in *Waste*, Elsevier, New York **2019**, pp. 381–404.
[10] V. Karthikeyan, J. U. Surjadi, J. C. K. Wong, V. Kannan, K. H. Lam, X. Chen, Y. Lu, V. A. L. Roy, *J. Power Sources* **2020**, *455*, 227983.
[11] S. M. Pourkiaei, M. H. Ahmadi, M. Sadeghzadeh, S. Moosavi, F. Pourfayaz, L. Chen, M. A. Pour Yazdi, R. Kumar, *Energy* **2019**, *186*, 115849.
[12] A. Nozariasbmarz, H. Collins, K. Dsouza, M. H. Polash, M. Hosseini, M. Hyland, J. Liu, A. Malhotra, F. M. Ortiz, F. Mohaddes, V. P. Ramesh, Y. Sargolzaeiaval, N. Snouwaert, M. C. Özturk, D. Vashaee, *Appl. Energy* **2019**, 114069.
[13] S. Shittu, G. Li, Y. G. Akhlaghi, X. Ma, X. Zhao, E. Ayodele, *Renewable Sustainable Energy Rev.* **2019**, *109*, 24.
[14] D. D. L. Chung, *Adv. Ind. Eng. Polym. Res.* **2018**, *1*, 61.
[15] C. K. Chiang, C. R. Fincher, Y. W. Park, A. J. Heeger, H. Shirakawa, E. J. Louis, S. C. Gau, A. G. MacDiarmid, *Phys. Rev. Lett.* **1977**, *39*, 1098.
[16] H. Wang, C. Yu, *Joule* **2019**, *3*, 53.
[17] Z. Qiu, B. A. G. Hammer, K. Müllen, *Prog. Polym. Sci.* **2020**, *100*, 101179.
[18] D. Beretta, N. Neophytou, J. M. Hodges, M. G. Kanatzidis, D. Narducci, M. Martin-Gonzalez, M. Beekman, B. Balke, G. Cerretti, W. Tremel, A. Zevalkink, A. I. Hofmann, C. Müller, B. Dörling, M. Campoy-Quiles, M. Caironi, *Mater. Sci. Eng., R* **2019**, *138*, 100501.
[19] S. Qu, Q. Yao, L. Wang, J. Hua, L. Chen, *Polymer* **2018**, *136*, 149.
[20] K. Wei, G. S. Nolas, *Scr. Mater.* **2018**, *150*, 70.
[21] M. Bharti, A. Singh, S. Samanta, D. K. Aswal, *Prog. Mater. Sci.* **2018**, *93*, 270.
[22] L. Chen, W. Liu, Y. Yan, X. Su, S. Xiao, X. Lu, C. Uher, X. Tang, *J. Mater. Chem. C* **2019**, *7*, 2333.
[23] D. Milić, A. Prijić, L. Vračar, Z. Prijić, *Appl. Therm. Eng.* **2017**, *121*, 74.
[24] C. Wei, L. Wang, C. Pan, Z. Chen, H. Zhao, L. Wang, *React. Funct. Polym.* **2019**, *142*, 1.
[25] K. Kang, S. Schott, D. Venkateshvaran, K. Broch, G. Schweicher, D. Harkin, C. Jellett, C. B. Nielsen, I. McCulloch, H. Sirringhaus, *Mater. Today Phys.* **2019**, *8*, 112.
[26] A. M. Darwish, A. Muhammad, S. S. Sarkisov, P. Mele, P. Saini, J. Liu, J. Shiomi, *Composites, Part B* **2019**, *167*, 406.
[27] M. Aghelinejad, S. N. Leung, *Composites, Part B* **2018**, *145*, 100.
[28] P. Huang, B. Copertaro, X. Zhang, J. Shen, I. Löfgren, M. Rönnelid, J. Fahlen, D. Andersson, M. Svanfeldt, *Appl. Energy* **2020**, *258*, 114109.
[29] K. Choi, S. L. Kim, S. Yi, J.-H. Hsu, C. Yu, *ACS Appl. Mater. Interfaces* **2018**, *10*, 23891.
[30] S. L. Kim, J.-H. Hsu, C. Yu, *Org. Electron.* **2018**, *54*, 231.
[31] J.-Y. Kim, W. Lee, Y. H. Kang, S. Y. Cho, K.-S. Jang, *Carbon* **2018**, *133*, 293.
[32] K. Yusupov, A. Zakhidov, S. You, S. Stumpf, P. M. Martinez, A. Ishteev, A. Vomiero, V. Khovaylo, U. Schubert, *J. Alloys Compd.* **2018**, *741*, 392.

**ADVANCED
SCIENCE NEWS**

www.advancedsciencenews.com

**ADVANCED
FUNCTIONAL
MATERIALS**

www.afm-journal.de

[33] K. Yusupov, S. You, A. Vomiero, A. Zakhidov, V. Khovaylo, S. Stumpf, U. S. Schubert, A. Bogach, P. M. Martinez, *Adv. Funct. Mater.* **2018**, *28*, 1870285.

[34] S. Liu, H. Li, C. He, *Carbon* **2019**, *149*, 25.

[35] Y. Gelbstein, *J. Appl. Phys.* **2009**, *105*, 023713.

[36] Q. Jiang, X. Lan, C. Liu, H. Shi, Z. Zhu, F. Zhao, J. Xu, F. Jiang, *Mater. Chem. Front.* **2018**, *2*, 679.

[37] S. Liu, J. Kong, H. Chen, C. He, *ACS Appl. Energy Mater.* **2019**, *2*, 8843.

[38] C. Gayner, Y. Amouyal, *Adv. Funct. Mater.* **2020**, *30*, 1901789.

[39] X. Zhao, X. Zhu, R. Zhang, *Phys. Status Solidi* **2016**, *213*, 3250.

[40] L. Ji, in *Metal Oxides in Energy Technologies*, Elsevier, New York **2018**, pp. 49–72.

[41] A. K. Yusupov, D. Hedman, A. P. Tsapenko, A. Ishteev, S. You, V. Khovaylo, A. Larsson, A. G. Nasibulin, A. Vomiero, *J. Alloys Compd.* **2020**, *845*, 156354.

[42] L. Wang, J. Zhang, Y. Guo, X. Chen, X. Jin, Q. Yang, K. Zhang, S. Wang, Y. Qiu, *Carbon* **2019**, *148*, 290.

[43] D. L. Stevens, A. Parra, J. C. Grunlan, *ACS Appl. Energy Mater.* **2019**, *2*, 5975.

[44] J. Y. Oh, G. H. Jun, S. Jin, H. J. Ryu, S. H. Hong, *ACS Appl. Mater. Interfaces* **2016**, *8*, 3319.

[45] X. Liu, Y. Du, Q. Meng, S. Z. Shen, J. Xu, *J. Mater. Sci.: Mater. Electron.* **2019**, *30*, 20369.

[46] Y. Lu, Y. Qiu, Q. Jiang, K. Cai, Y. Du, H. Song, M. Gao, C. Huang, J. He, D. Hu, *ACS Appl. Mater. Interfaces* **2018**, *10*, 42310.

[47] M. Martín-González, O. Caballero-Calero, P. Díaz-Chao, *Renewable Sustainable Energy Rev.* **2013**, *24*, 288.

[48] H. Ju, D. Park, J. Kim, *Nanoscale* **2019**, *11*, 16114.

[49] D. Ni, H. Song, Y. Chen, K. Cai, *J. Mater.* **2020**, *6*, 364.

[50] D. Lee, J. Zhou, G. Chen, Y. Shao-Horn, *Adv. Electron. Mater.* **2019**, *5*, 1800624.

[51] K. H. Lim, K. W. Wong, D. Cadavid, Y. Liu, Y. Zhang, A. Cabot, K. M. Ng, *Composites, Part B* **2019**, *164*, 54.

[52] W. S. Kim, G. Anoop, I.-S. Jeong, H. J. Lee, H. Bin Kim, S. H. Kim, G. W. Goo, H. Lee, H. J. Lee, C. Kim, J.-H. Lee, B. S. Mun, J.-W. Park, E. Lee, J. Y. Jo, *Nano Energy* **2020**, *67*, 104207.

[53] T. G. Novak, H. Shin, J. Kim, K. Kim, A. Azam, C. V. Nguyen, S. H. Park, J. Y. Song, S. Jeon, *ACS Appl. Mater. Interfaces* **2018**, *10*, 17957.

[54] J.-Y. Lee, Y.-J. Lin, *Synth. Met.* **2016**, *212*, 180.

[55] W. Shi, S. Qu, H. Chen, Y. Chen, Q. Yao, L. Chen, *Angew. Chem., Int. Ed.* **2018**, *57*, 8037.

[56] O. Bubnova, Z. U. Khan, H. Wang, S. Braun, D. R. Evans, M. Fabretto, P. Hojati-Talemi, D. Dagnelund, J.-B. Arlin, Y. H. Geerts, S. Desbief, D. W. Breiby, J. W. Andreasen, R. Lazzaroni, W. M. Chen, I. Zozoulenko, M. Fahlman, P. J. Murphy, M. Berggren, X. Crispin, *Nat. Mater.* **2014**, *13*, 190.

[57] W. Thongkham, C. Lertsatitthanakorn, K. Jiramitmongkon, K. Tantisantisom, T. Boonkoom, M. Jitpukdee, K. Sinthiptharakoon, A. Klamchuen, M. Liangruksa, P. Khanchaitit, *ACS Appl. Mater. Interfaces* **2019**, *11*, 6624.

[58] Y. Lu, Y. Ding, Y. Qiu, K. Cai, Q. Yao, H. Song, L. Tong, J. He, L. Chen, *ACS Appl. Mater. Interfaces* **2019**, *11*, 12819.

[59] L. Peng, Z. Liu, *J. Mater. Chem. C* **2019**, *7*, 6120.

[60] Z. Fan, D. Du, X. Guan, J. Ouyang, *Nano Energy* **2018**, *51*, 481.

[61] Z. Fan, P. Li, D. Du, J. Ouyang, *Adv. Energy Mater.* **2017**, *7*, 1602116.

[62] H. Jia, X. Tao, Y. Wang, *Adv. Electron. Mater.* **2016**, *2*, 1600136.

[63] D. B. Ingham, I. Pop, *Transport Phenomena in Porous Media III*, Elsevier, New York **2005**.

[64] C. J. Wienken, P. Baaske, U. Rothbauer, D. Braun, S. Duhr, *Nat. Commun.* **2010**, *1*, 100.

[65] M. A. Rahman, M. Z. Saghir, *Int. J. Heat Mass Transfer* **2014**, *73*, 693.

[66] X. Guan, H. Cheng, J. Ouyang, *J. Mater. Chem. A* **2018**, *6*, 19347.

[67] N. Saxena, B. Pretzl, X. Lamprecht, L. Bießmann, D. Yang, N. Li, C. Bilko, S. Bernstorff, P. Müller-Buschbaum, *ACS Appl. Mater. Interfaces* **2019**, *11*, 8060.

[68] B. Kim, J. Na, H. Lim, Y. Kim, J. Kim, E. Kim, *Adv. Funct. Mater.* **2019**, *29*, 1807549.

[69] C. Wang, K. Sun, J. Fu, R. Chen, M. Li, Z. Zang, X. Liu, B. Li, H. Gong, J. Ouyang, *Adv. Sustainable Syst.* **2018**, *2*, 1800085.

[70] H. Yao, Z. Fan, P. Li, B. Li, X. Guan, D. Du, J. Ouyang, *J. Mater. Chem. A* **2018**, *6*, 24496.

[71] A. Mazaheripour, S. Majumdar, D. Hanemann-Rawlings, E. M. Thomas, C. McGuiness, L. d'Alencon, M. L. Chabinyc, R. A. Segalman, *Chem. Mater.* **2018**, *30*, 4816.

[72] M. T. Zar Myint, M. Hada, H. Inoue, T. Marui, T. Nishikawa, Y. Nishina, S. Ichimura, M. Umeno, A. K. Ko Kyaw, Y. Hayashi, *RSC Adv.* **2018**, *8*, 36563.

[73] X. Li, C. Liu, W. Zhou, X. Duan, Y. Du, J. Xu, C. Li, J. Liu, Y. Jia, P. Liu, Q. Jiang, C. Luo, C. Liu, F. Jiang, *ACS Appl. Mater. Interfaces* **2019**, *11*, 8138.

[74] D. Ni, H. Song, Y. Chen, K. Cai, *Energy* **2019**, *170*, 53.

[75] M. Tonga, L. Wei, E. Wilusz, L. Korugic-Karasz, F. E. Karasz, P. M. Lahti, *Synth. Met.* **2018**, *239*, 51.

[76] Y. H. Kang, U.-H. Lee, I. H. Jung, S. C. Yoon, S. Y. Cho, *ACS Appl. Electron. Mater.* **2019**, *1*, 1282.

[77] E. Jang, A. Poosapati, D. Madan, *ACS Appl. Energy Mater.* **2018**, *1*, 1455.

[78] L. Sun, G. Xie, P. Wu, Y. Xiong, L. Xu, *ACS Appl. Polym. Mater.* **2019**, *1*, 1054.

[79] J. Hynynen, D. Kiefer, C. Müller, *RSC Adv.* **2018**, *8*, 1593.

[80] E. Lim, K. A. Peterson, G. M. Su, M. L. Chabinyc, *Chem. Mater.* **2018**, *30*, 998.

[81] E. Lim, A. M. Glaudell, R. Miller, M. L. Chabinyc, *Adv. Electron. Mater.* **2019**, *5*, 1800915.

[82] Y. Zou, D. Huang, Q. Meng, C. Di, D. Zhu, *Org. Electron.* **2018**, *56*, 125.

[83] V. Vijayakumar, Y. Zhong, V. Untilova, M. Bahri, L. Herrmann, L. Biniek, N. Leclerc, M. Brinkmann, *Adv. Energy Mater.* **2019**, *9*, 1900266.

[84] J. Hynynen, E. Järsvall, R. Kroon, Y. Zhang, S. Barlow, S. R. Marder, M. Kemerink, A. Lund, C. Müller, *ACS Macro Lett.* **2019**, *8*, 70.

[85] H. Li, S. Liu, P. Li, D. Yuan, X. Zhou, J. Sun, X. Lu, C. He, *Carbon* **2018**, *136*, 292.

[86] R. Wu, H. Yuan, C. Liu, J. Le Lan, X. Yang, Y. H. Lin, *RSC Adv.* **2018**, *8*, 26011.

[87] Y.-H. Lin, T.-C. Lee, Y.-S. Hsiao, W.-K. Lin, W.-T. Whang, C.-H. Chen, *ACS Appl. Mater. Interfaces* **2018**, *10*, 4946.

[88] S. Wang, F. Liu, C. Gao, T. Wan, L. Wang, L. Wang, L. Wang, *Chem. Eng. J.* **2019**, *370*, 322.

[89] J. Xie, X. Wang, S. Wang, Z. Ling, H. Lian, N. Liu, Y. Liao, X. Yang, W. Qu, Y. Peng, W. Lan, B. Wei, *Org. Electron.* **2019**, *75*, 105381.

[90] D. Mombrú, M. Romero, R. Faccio, A. W. Mombrú, *J. Mater. Sci. Mater. Electron.* **2018**, *29*, 17445.

[91] H. Li, Y. Liang, S. Liu, F. Qiao, P. Li, C. He, *Org. Electron.* **2019**, *69*, 62.

[92] F. P. Du, Q. Q. Li, P. Fu, Y. F. Zhang, Y. G. Wu, *J. Mater. Sci. Mater. Electron.* **2018**, *29*, 8666.

[93] F. Erden, H. Li, X. Wang, F. K. Wang, C. He, *Phys. Chem. Chem. Phys.* **2018**, *20*, 9411.

[94] H. Ju, D. Park, J. Kim, *ACS Appl. Mater. Interfaces* **2018**, *10*, 11920.

[95] M. Mitra, C. Kulsi, K. Kargupta, S. Ganguly, D. Banerjee, *J. Appl. Polym. Sci.* **2018**, *135*, 46887.

[96] Y. Wang, C. Yu, G. Liu, M. Sheng, Y. Deng, *Mater. Lett.* **2018**, *229*, 293.

[97] Y. Wang, G. Liu, M. Sheng, C. Yu, Y. Deng, *J. Mater. Chem. A* **2019**, *7*, 1718.

**ADVANCED
SCIENCE NEWS**

www.advancedsciencenews.com

**ADVANCED
FUNCTIONAL
MATERIALS**

www.afm-journal.de

[98] K. Sarkar, A. Debnath, K. Deb, A. Bera, B. Saha, *Energy* **2019**, *177*, 203.

[99] C.-C. Lin, Y.-C. Huang, M. Usman, W.-H. Chao, W.-K. Lin, T.-T. Luo, W.-T. Whang, C.-H. Chen, K.-L. Lu, *ACS Appl. Mater. Interfaces* **2019**, *11*, 3400.

[100] M. H. Penteado, I. Cruz-Cruz, I. A. Hümmelgen, *Org. Electron.* **2019**, *67*, 153.

[101] L. Horta-Romarís, M. V. González-Rodríguez, A. Lasagabáster, F. Rivadulla, M. J. Abad, *Synth. Met.* **2018**, *243*, 44.

[102] Y. Jia, L. Shen, J. Liu, W. Zhou, Y. Du, J. Xu, C. Liu, G. Zhang, Z. Zhang, F. Jiang, *J. Mater. Chem. C* **2019**, *7*, 3496.

[103] K. Zhang, S. Wang, J. Qiu, J. L. Blackburn, X. Zhang, A. J. Ferguson, E. M. Miller, B. L. Weeks, *Nano Energy* **2016**, *19*, 128.

[104] O. Bubnova, X. Crispin, *Energy Environ. Sci.* **2012**, *5*, 9345.

Khabib Yusupov received his B.Sc. degree (2012) in polymer chemistry from Saratov State Technical University. After graduating at NUST MISiS with M.Sc. degree (2014) in nanomaterial physics, he was further admitted for Ph.D. education. Currently, he is working as a postdoctoral researcher at the Luleå University of Technology, Sweden. His research focuses on thermoelectric properties of organic and inorganic materials.

Alberto Vomiero is a chair professor in Experimental Physics at the Department of Engineering Sciences and Mathematics, Luleå University of Technology, Sweden, and a professor in Industrial Engineering at the Department of Molecular Sciences and Nanosystems, Ca' Foscari University of Venice, Italy. He is leading a multidisciplinary group focusing on the development of advanced nanomaterials for energy and environmental applications, including solar cells, water splitting, and photocatalysis.